# Własności neutronowo nadmiarowych izotopów z obszaru od niobu do srebra, o liczbach masowych 107 – 119; w tym zagadki rozpadu beta, własności stanów izomerycznych, deformacje stanów jądrowych. Wyniki badań eksperymentalnych wykonanych w Laboratorium Cyklotronowym Uniwersytetu w Jyvaskyla

Plan seminarium

0. Motywacja
1. Krótkie omówienie metod eksperymentalnych
2. Podsumowanie dotychczasowych badań
3. Wyniki badań rozpadu beta $^{117}$Rh -> $^{117}$Pd
4. Rozpad beta izotopów omawianego obszaru
5. Własności stanów wzbudzonych izotopów palladu o liczbach masowych 110 – 117
6. Deformacja izotopów palladu
7. Przygotowywane publikacje i plany na przyszłość

ELSEVIER

Nuclear Physics A 617 (1997) 282–315

NUCLEAR PHYSICS A

# Equilibrium shapes and high-spin properties of the neutron-rich $A \approx 100$ nuclei

J. Skalski [a,b], S. Mizutori [a,c], W. Nazarewicz [c,d,e]

[a] Joint Institute for Heavy-Ion Research, Oak Ridge National Laboratory, P.O. Box 2008, Oak Ridge, TN 37831, USA
[b] Sołtan Institute for Nuclear Studies, ul. Hoża 69, PL-00681 Warsaw, Poland
[c] Physics Division, Oak Ridge National Laboratory, P.O. Box 2008, Oak Ridge, TN 37831, USA
[d] Department of Physics and Astronomy, University of Tennessee, Knoxville, TN 37996, USA
[e] Institute of Theoretical Physics, Warsaw University, ul. Hoża 69, PL-00681 Warsaw, Poland

Received 19 February 1997

Equilibrium deformations and moments, potential energy surfaces, microscopic structure of coexisting configurations, and shape transitions in the heavy-Zr region have been calculated by many authors [35–85]. In most cases, calculations show large deformations in Sr, Zr, and Mo isotopes with $N \geqslant 60$. However, the details of the shape transition near $N = 58$ is predicted differently by various models, the onset and rapidity of this transition being very sensitive to the model [2].



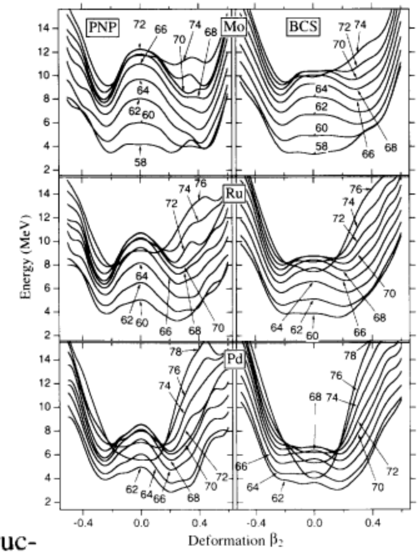




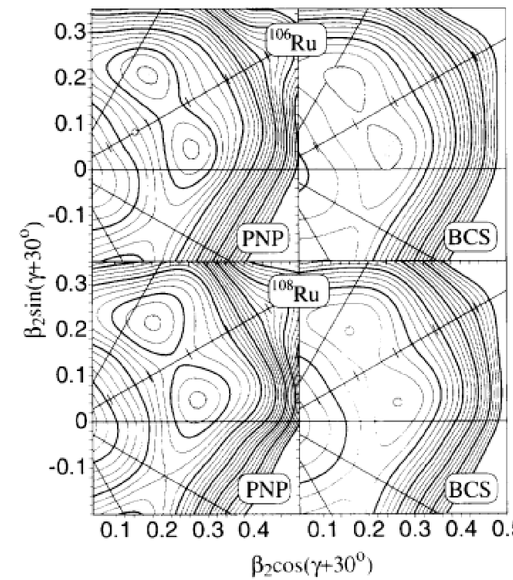


Eur. Phys. J. A **24**, 161–165 (2005)
DOI 10.1140/epja/i2004-10140-7

THE EUROPEAN PHYSICAL JOURNAL A

*Letter*

# First observation of excited states in the $^{111}$Tc nucleus —A new region of deformation at $40 \leq Z \leq 46$, $N \geq 68$?

W. Urban[1,a], T. Rząca-Urban[1], J.L. Durell[2], A.G. Smith[2], and I. Ahmad[3]

[1] Faculty of Physics, Warsaw University, ul. Hoża 69, 00-681 Warsaw, Poland
[2] Department of Physics and Astronomy, University of Manchester, Manchester M13 9PL, UK
[3] Argonne National Laboratory, Argonne, IL 60439, USA

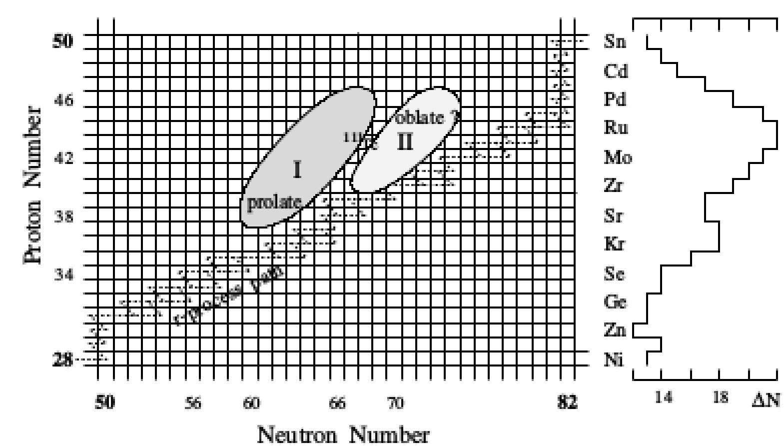


**Fig. 1.** Approximate regions of nuclear deformations and the approximate position of the r-process path in the $28 < Z < 50$, $50 < N < 82$ region. To the right, the distance, $\Delta N$, from the stability line to the path, is shown for various isotopes.

PHYSICAL REVIEW C, VOLUME 65, 021303 (2001)
Oblate stability of A~110 nuclei near the r-process path

F. R. XU, P. M. WALKER, AND R. WYSS

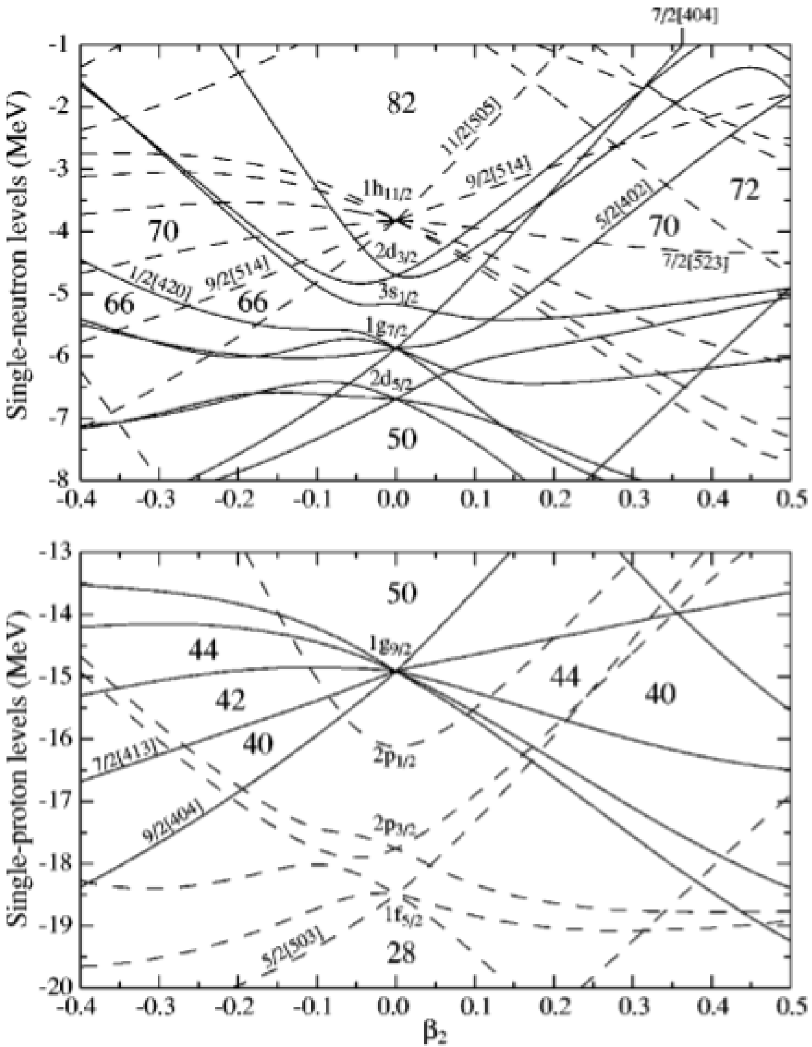


FIG. 1. The calculated single-neutron (top) and single-proton (bottom) levels of the Woods-Saxon potential. Axial symmetry is assumed with $\beta_4 = -|\beta_2|/6$ which gives approximately the hexadecapole value of the ground states obtained from the TRS calculations. Positive (negative) parity is indicated by solid (dashed) lines.

Even-even A ≈ 110 nuclei approaching the astrophysical r-process path have been investigated using both the cranked and the configuration-constrained shell models.
The calculations show that, with increasing neutron number in the Z ≥ 40 nuclides, nuclear shapes evolve from prolate, through triaxial to oblate deformations.

# NuDat 2.7

Search and plot nuclear structure and decay data interactively. More.

Levels and Gammas Search
Ground and excited states (energy, $T_{1/2}$, spin/parity, decay modes), gamma rays (energy, intensity, multipolarity, coinc.)

Nuclear Wallet Cards Search
Latest Ground and isomeric states properties

Decay
Radiat
intensi
followi

| Color code | Half-life | Decay Mode | $Q_{\beta-}$ | $Q_{EC}$ | $Q_{\beta+}$ | $S_n$ | $S_p$ | $Q_\alpha$ | $\Delta Q_\alpha$ | $S_{2n}$ | $S_{2p}$ | $Q_{2\beta-}$ | $Q_{2EC}$ |
|---|---|---|---|---|---|---|---|---|---|---|---|---|---|
| $Q_{\beta-2n}$ | BE/A | (BE-LDM Fit)/A | Pair. gap | $E_{1st\ ex.\ st.}$ | $E_{2+}$ | $E_{3-}$ | $E_{4+}$ | $E_{4+}/E_{2+}$ | $\beta_2$ | $B(E2)_{42}/B(E2)_{20}$ | $\sigma(n,\gamma)$ | $\sigma(n,F)$ | 235U F |

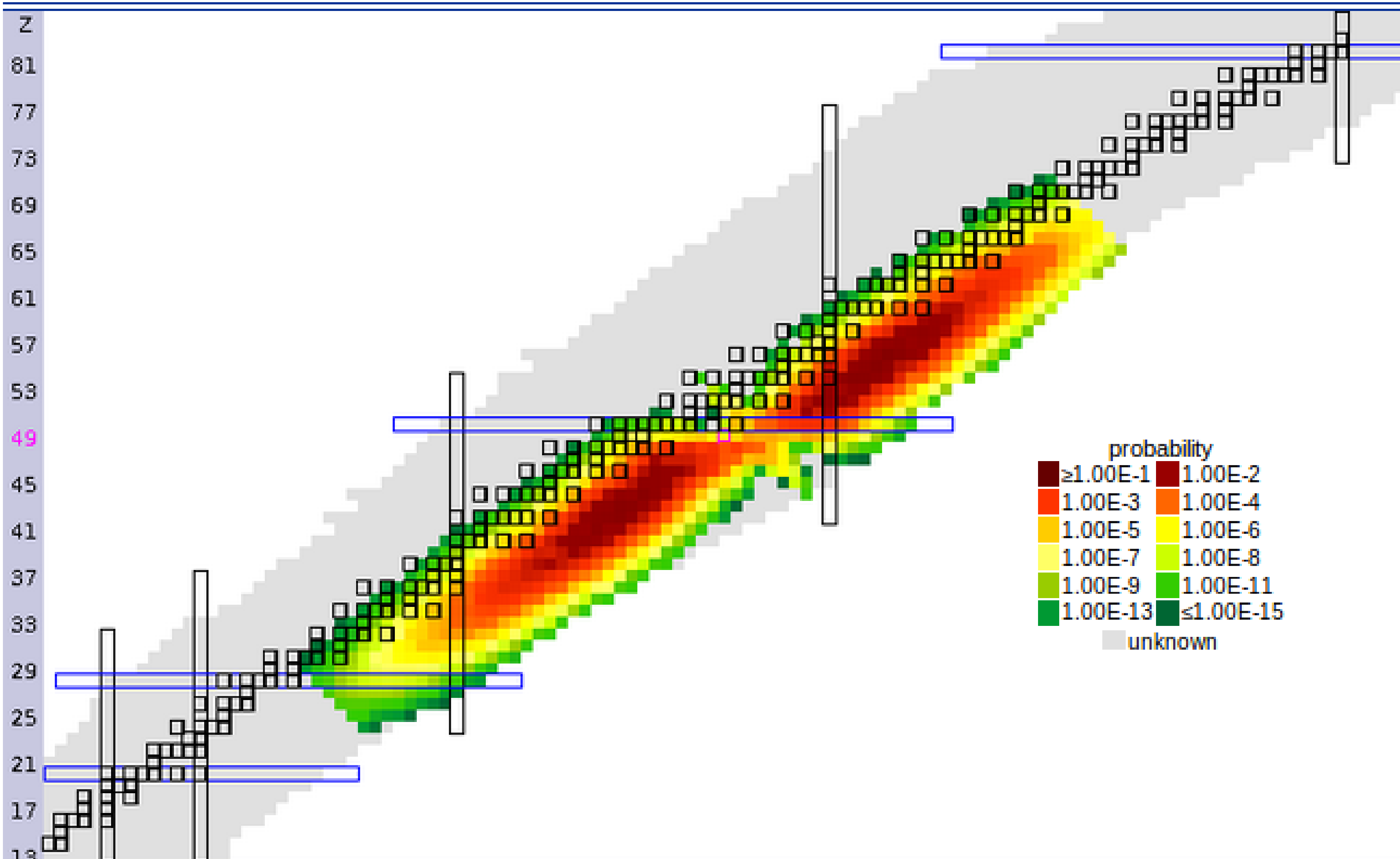

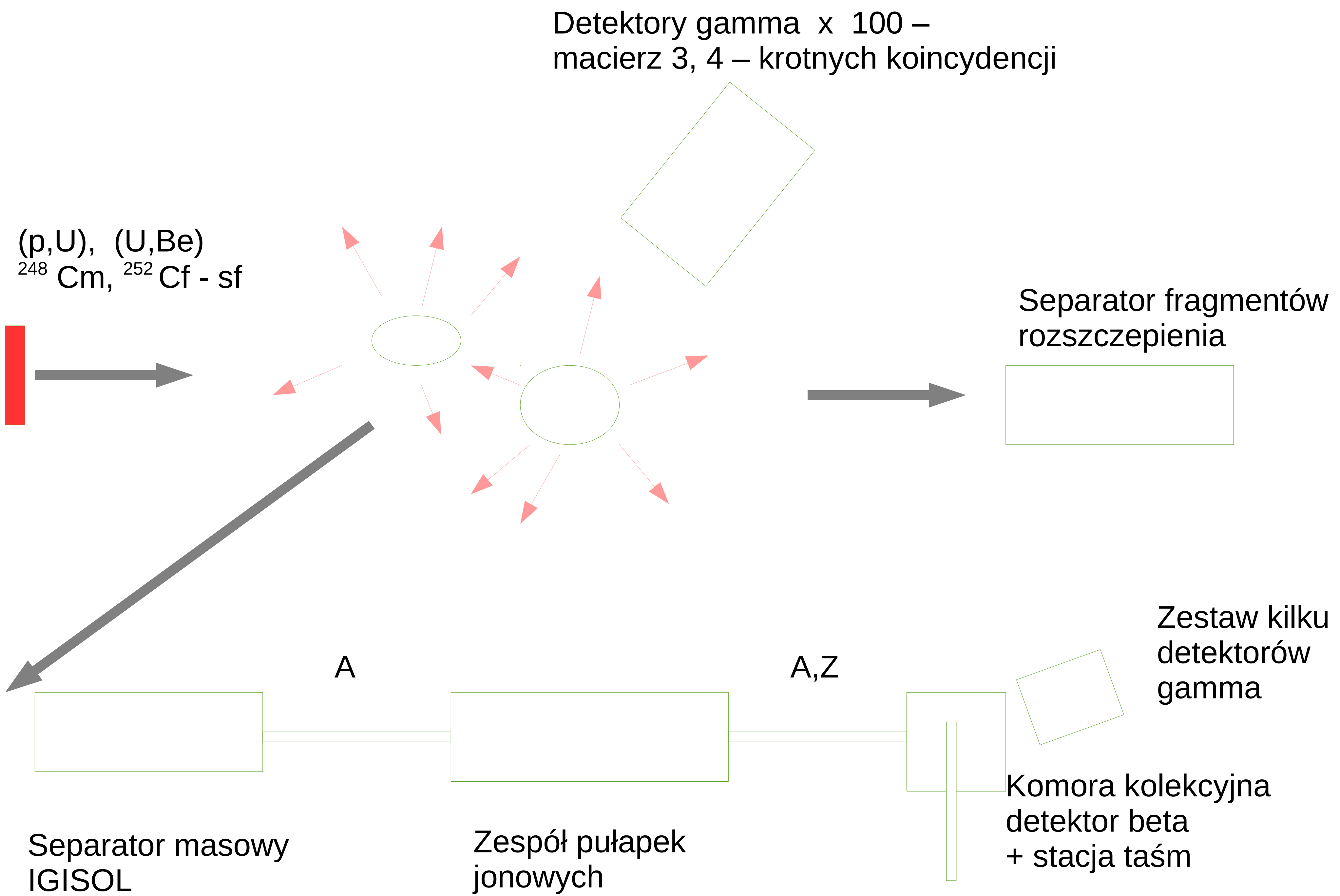

Detektory gamma x 100 –
macierz 3, 4 – krotnych koincydencji
(p,U), (U,Be)
248 Cm, 252 Cf - sf
Separator fragmentów
rozszczepienia
Zestaw kilku
detektorów
gamma
A
A,Z
Komora kolekcyjna
detektor beta
+ stacja taśm
Separator masowy
IGISOL
Zespół pułapek
jonowych

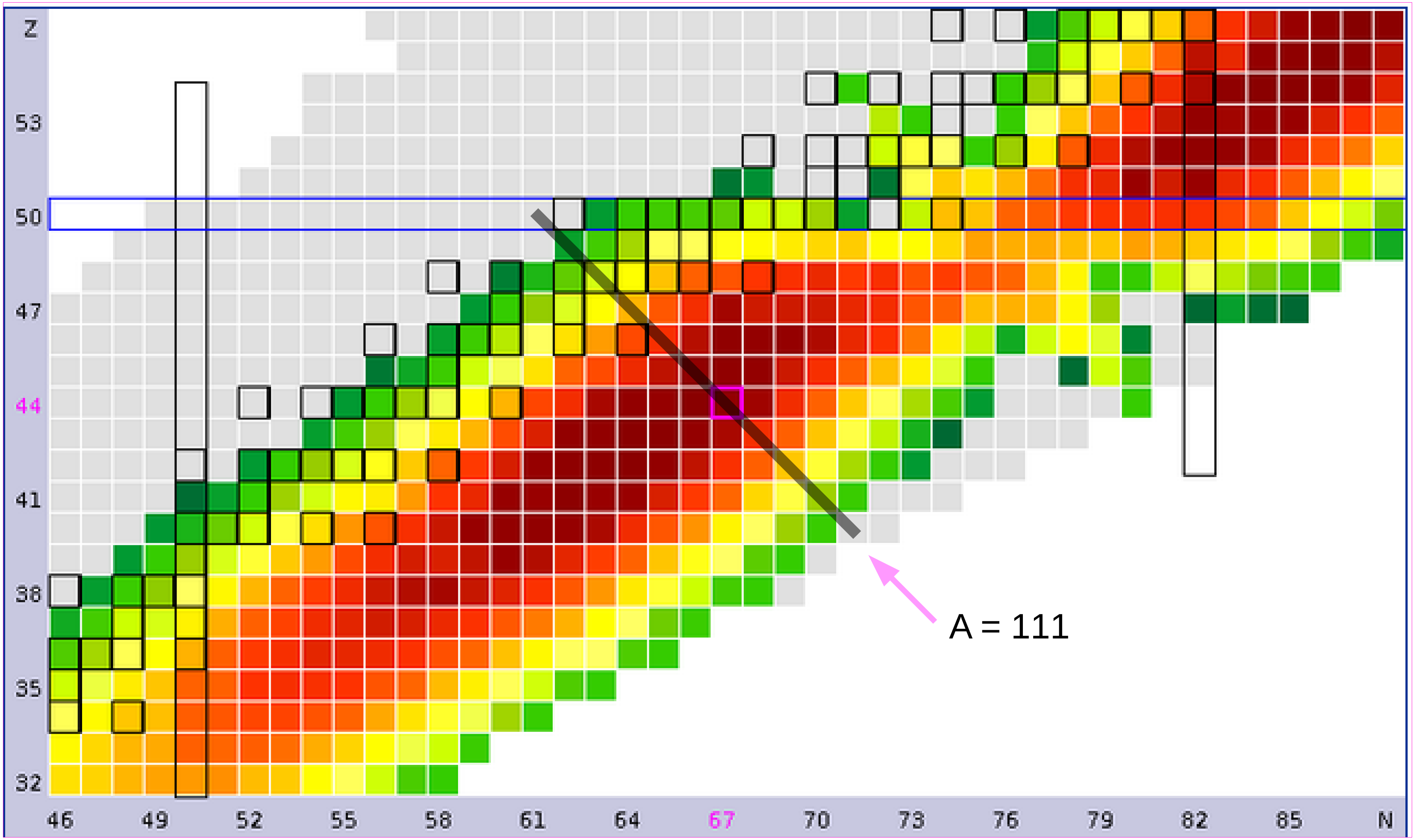
Z
53
50
47
44
41
38
35
32
46
49
52
55
58
61
64
67
70
73
76
79
82
85
N
A = 111

$_{44}Ru_{67}$

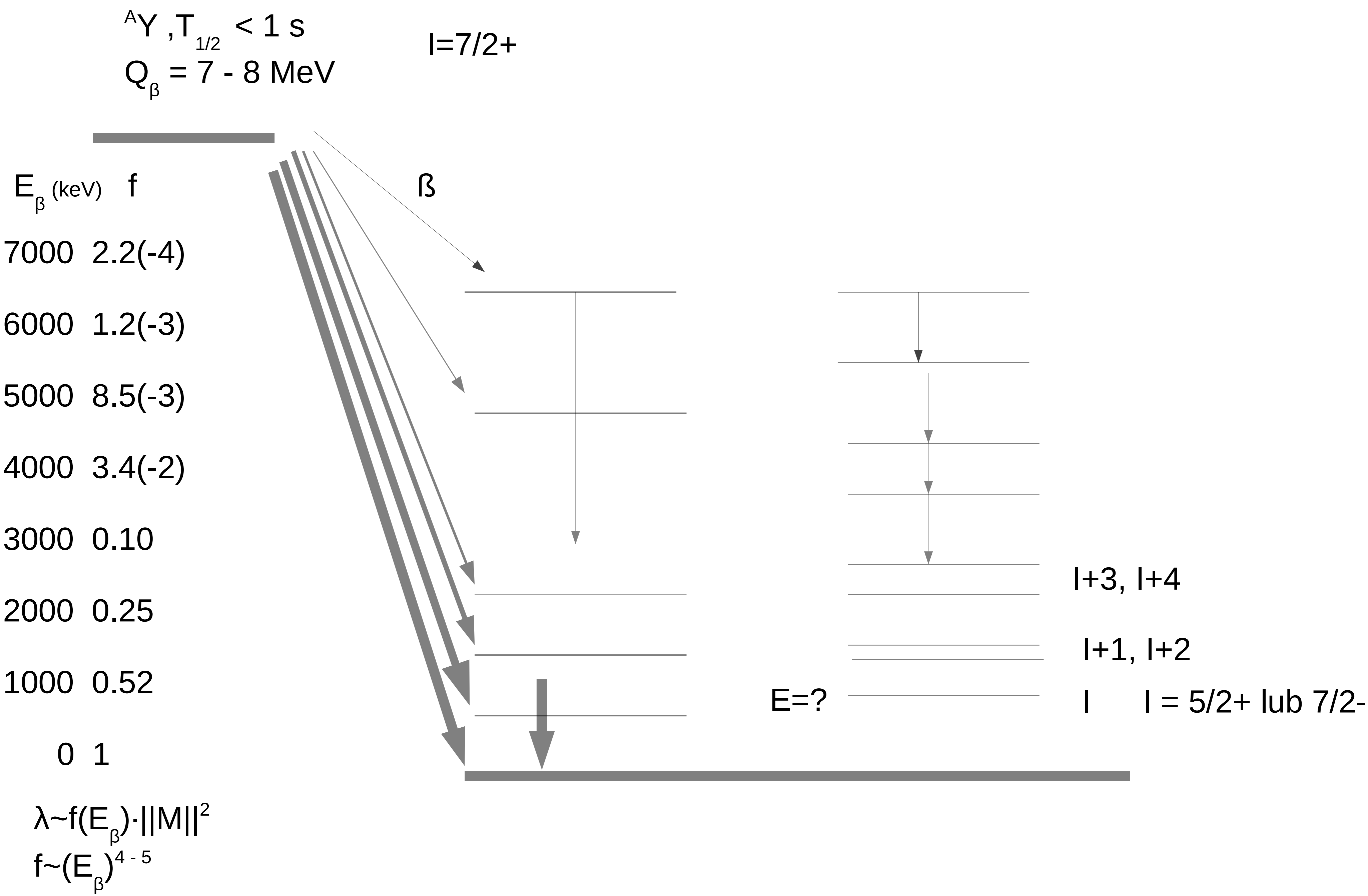
$^{A}Y$, $T_{1/2}$ < 1 s
$Q_{\beta}$ = 7 - 8 MeV
I=7/2+
ß
$E_{\beta}$ (keV) f
7000 2.2(-4)
6000 1.2(-3)
5000 8.5(-3)
4000 3.4(-2)
3000 0.10
2000 0.25
1000 0.52
0 1
I+3, I+4
I+1, I+2
E=?
I
I = 5/2+ lub 7/2-
$\lambda \sim f(E_{\beta})\cdot||M||^2$
$f \sim (E_{\beta})^{4-5}$

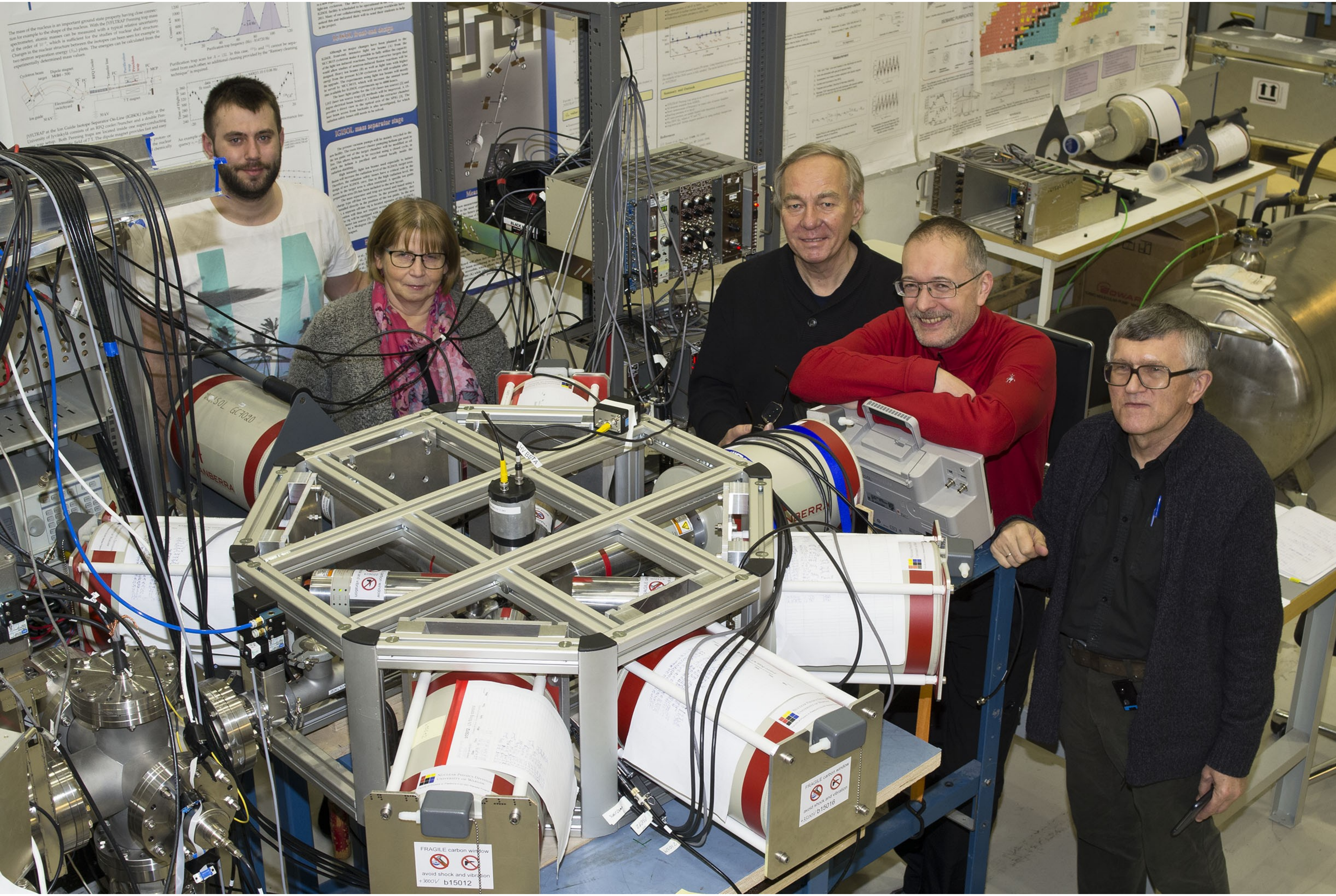
IGISOL mass separator stage
FRAGILE carbon window
avoid shock and vibration
b15012
b15016

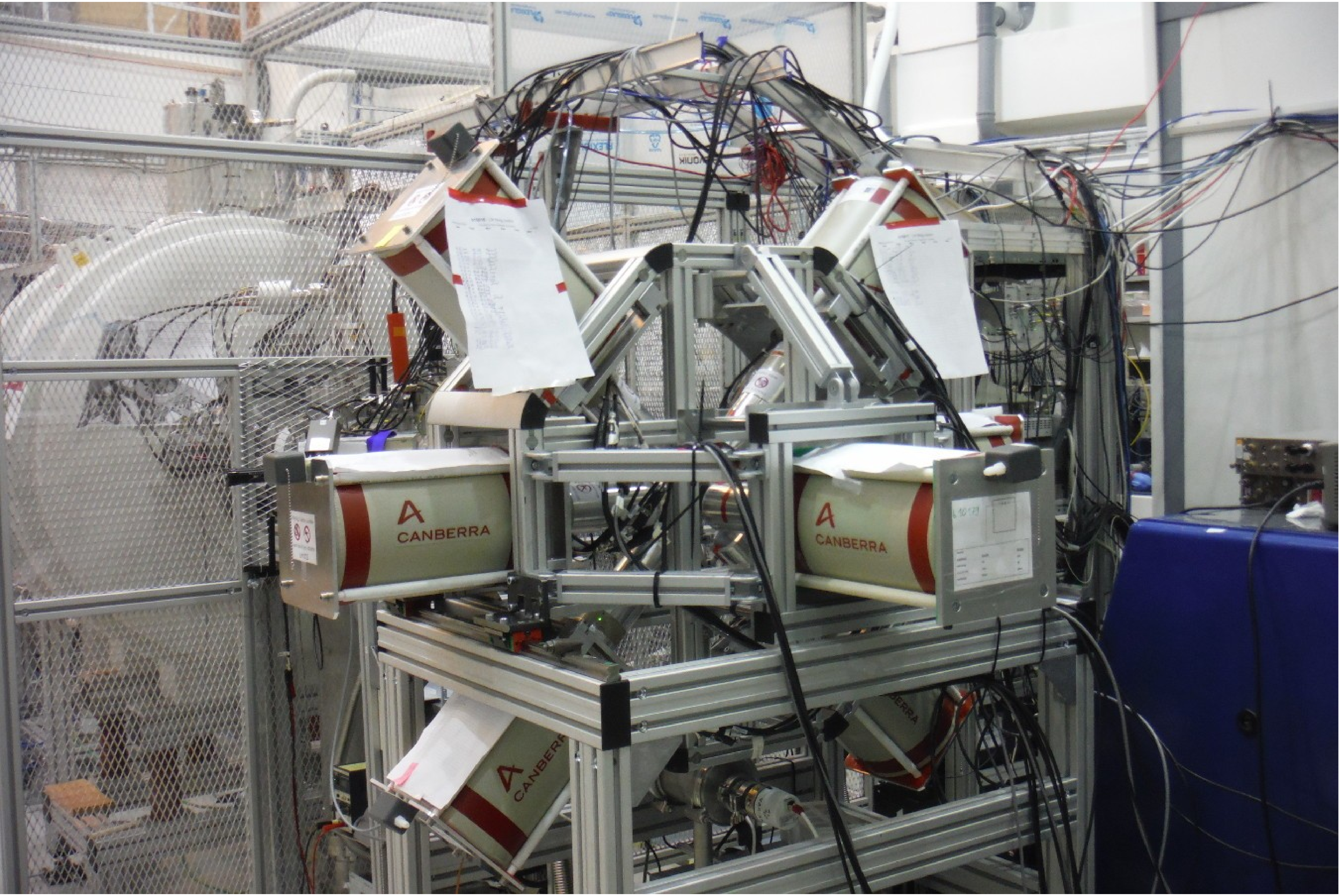
CANBERRA
CANBERRA
CANBERRA

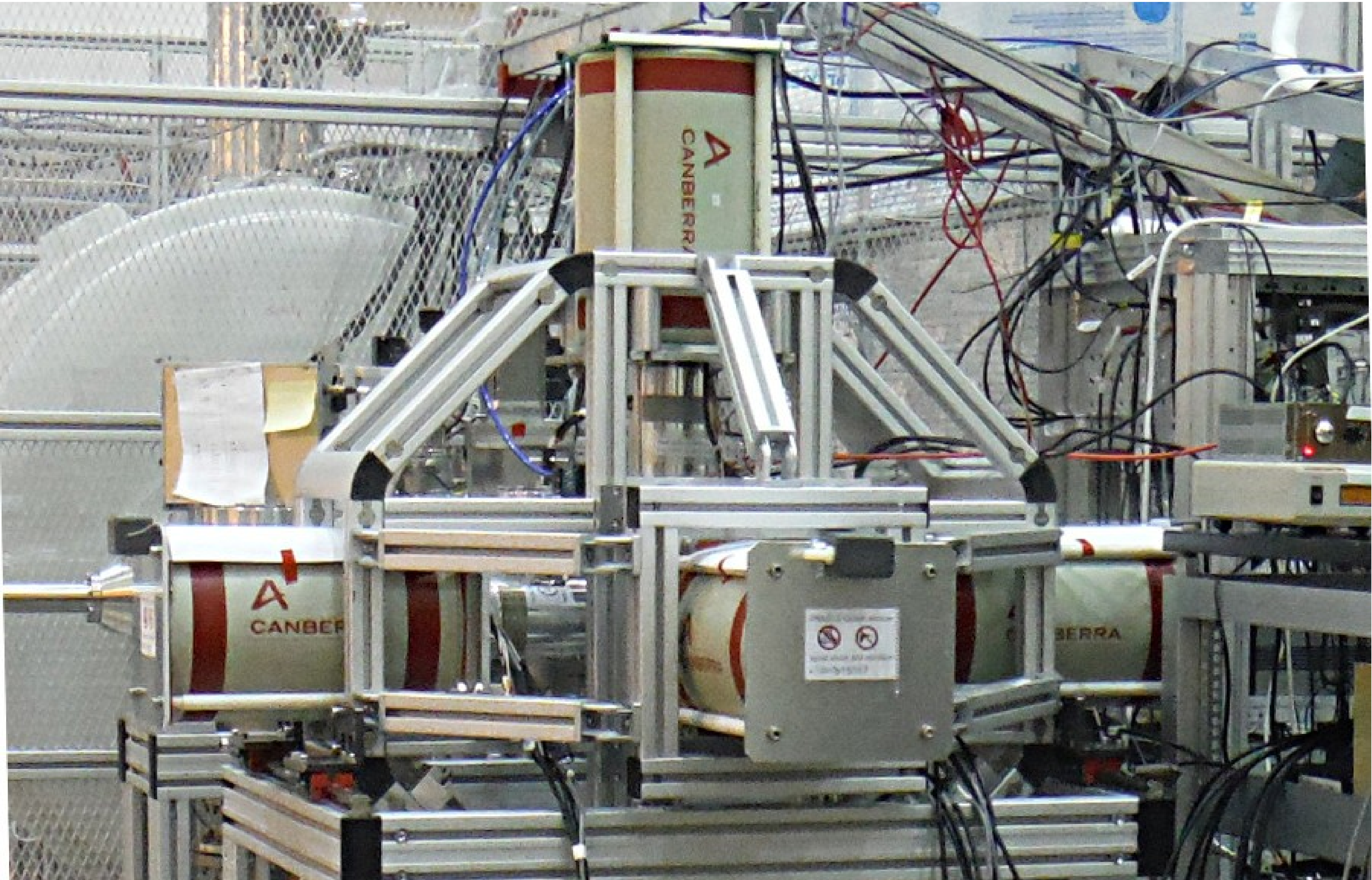
CANBERRA
CANBERRA

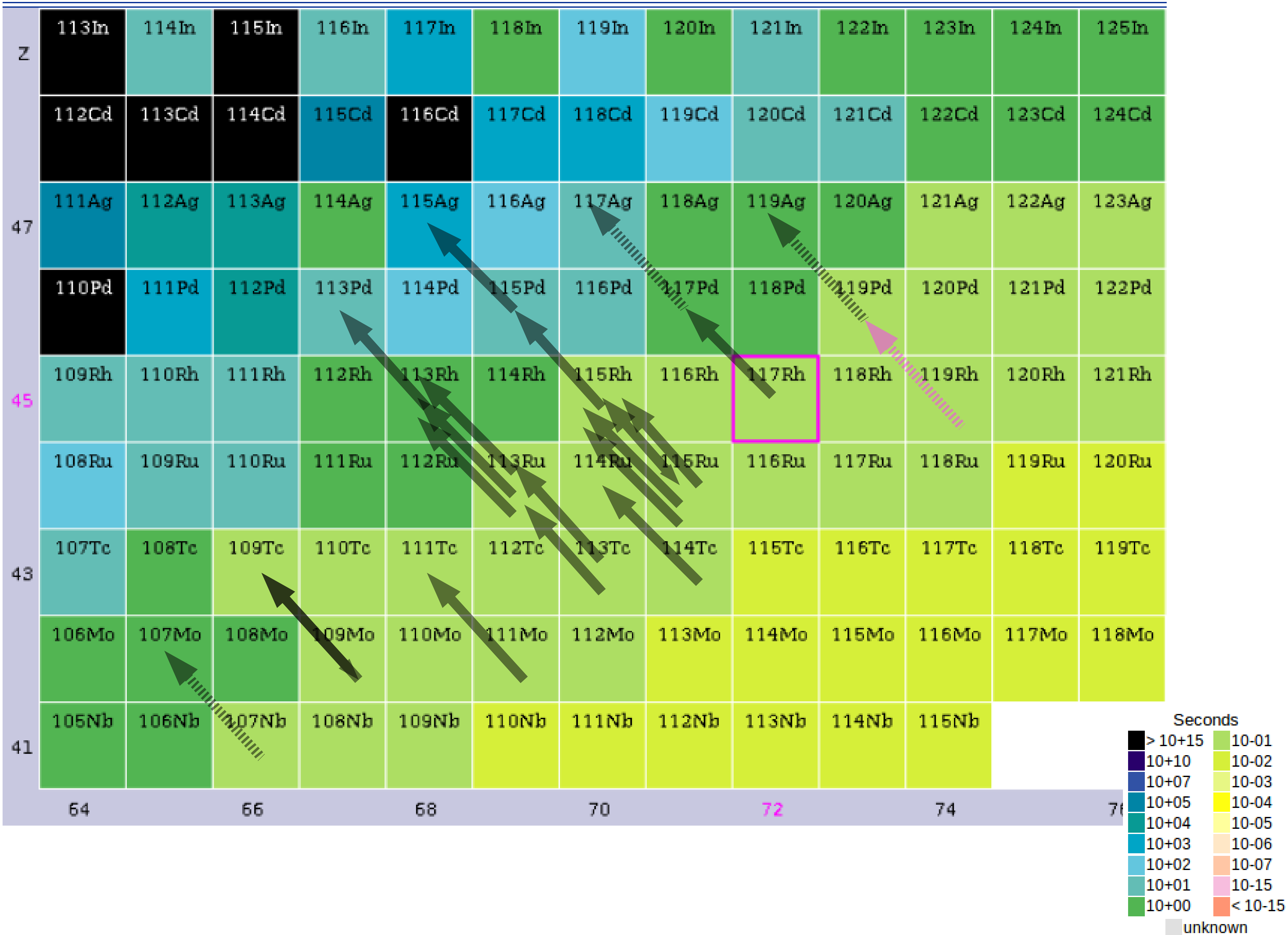

Z
47
45
43
41
64
66
68
70
72
74
113In 114In 115In 116In 117In 118In 119In 120In 121In 122In 123In 124In 125In
112Cd 113Cd 114Cd 115Cd 116Cd 117Cd 118Cd 119Cd 120Cd 121Cd 122Cd 123Cd 124Cd
111Ag 112Ag 113Ag 114Ag 115Ag 116Ag 117Ag 118Ag 119Ag 120Ag 121Ag 122Ag 123Ag
110Pd 111Pd 112Pd 113Pd 114Pd 115Pd 116Pd 117Pd 118Pd 119Pd 120Pd 121Pd 122Pd
109Rh 110Rh 111Rh 112Rh 113Rh 114Rh 115Rh 116Rh 117Rh 118Rh 119Rh 120Rh 121Rh
108Ru 109Ru 110Ru 111Ru 112Ru 113Ru 114Ru 115Ru 116Ru 117Ru 118Ru 119Ru 120Ru
107Tc 108Tc 109Tc 110Tc 111Tc 112Tc 113Tc 114Tc 115Tc 116Tc 117Tc 118Tc 119Tc
106Mo 107Mo 108Mo 109Mo 110Mo 111Mo 112Mo 113Mo 114Mo 115Mo 116Mo 117Mo 118Mo
105Nb 106Nb 107Nb 108Nb 109Nb 110Nb 111Nb 112Nb 113Nb 114Nb 115Nb
Seconds
> 10+15
10+10
10+07
10+05
10+04
10+03
10+02
10+01
10+00
10-01
10-02
10-03
10-04
10-05
10-06
10-07
10-15
< 10-15
unknown

**First decay scheme of $^{113}$Tc and identification of $^{113}$Ru$^{m}$**

J.Kurpeta, G. Lersonneau, J.C. Wang, P.Dendooven, A. Honkanen, M. Huhta, M. Oinonen,H. Penttilä, K. Peräjärvi, J.R. Persson,
A. Płochocki, J. Äystö
Eur. Phys. J A 2 (1998) 241-243

**Low-spin structure of $^{113}$Ru and $^{113}$Rh**

J. Kurpeta, W. Urban, Ch. Droste , A. Płochocki , S.G. Rohoziński , T. Rząca-Urban, T. Morek, L. Próchniak , Beta + sf + obliczenia
K. Starosta, J. Äystö , H. Penttilä, J.L. Durell , A.G. Smith, G. Lhersonneau, and I. Ahmad
Eur. Phys. J. A 33, 307–316 (2007)

**Penning trap assisted decay spectroscopy of neutron-rich $^{115}$Ru**

J. Kurpeta, V.-V. Elomaa, T. Eronen, J. Hakala, A. Jokinen, P. Karvonen, I. Moore, H. Penttila, Pierwszy pomiar z pułapką Penninga
A. Płochocki, S. Rahaman, S. Rinta-Antila, J. Rissanen, J. Ronkainen, A. Saastamoinen
T. Sonoda,W. Urban, Ch. Weber, and J. Aysto
Eur. Phys J. A 31 (2007) 263-266

**Signatures of oblate deformation in the $^{111}$Tc nucleus**

J. Kurpeta, W. Urban, A. Płochocki, J. Rissanen, J. A. Pinston, V.-V. Elomaa, T. Eronen,
J. Hakala, A. Jokinen, A. Kankainen, P. Karvonen, I. D. Moore, H. Penttila, A. Saastamoinen,
C. Weber and J. Aysto
Phys. Rev. C 84 (2011) 044304 1-4

**Decay study of $^{114}$Tc with a Penning trap**

J. Rissanen, J. Kurpeta, V.-V. Elomaa, T. Eronen, J. Hakala, A. Jokinen, I. D. Moore, P. Karvonen, A. Płochocki, L. Próchniak, H. Penttilä,
S. Rahaman, M. Reponen, A. Saastamoinen, J. Szerypo, W. Urban, C. Weber, and J. Äystö
Phys. Rev. C 83, 011301(R) – Published 7 January 2011;

doktorat

**Penning-trap-assisted study of excitations in $^{88}$Br populated in β decay of $^{88}$Se**

M. Czerwiński, K. Sieja, T. Rząca-Urban, W. Urban, A. Płochocki, J. Kurpeta, J. Wiśniewski, H. Penttilä, A. Jokinen, S. Rinta-Antila,
L. Canete, T. Eronen, J. Hakala, A. Kankainen, V. S. Kolhinen, J. Koponen, I. D. Moore, I. Pohjalainen, J. Reinikainen, V. Simutkin,
A. Voss, I. Murray, and C. Nobs
Phys. Rev. C 95, 024321 – Published 22 February 2017 Uzupełnienie doktoratu

PHYSICAL REVIEW C **98**, 024318 (2018)

# Excited levels in the multishaped $^{117}$Pd nucleus studied via $\beta$ decay of $^{117}$Rh

J. Kurpeta,[1] A. Płochocki,[1] W. Urban,[1] T. Eronen,[2] A. Jokinen,[2] A. Kankainen,[2] V. S. Kolhinen,[3] I. D. Moore,[2] H. Penttilä,[2] M. Pomorski,[1] S. Rinta-Antila,[2] T. Rząca-Urban,[1] and J. Wiśniewski[1]

[1]*Faculty of Physics, University of Warsaw, ul. Pasteura 5, PL-02-093 Warsaw, Poland*

[2]*Department of Physics, University of Jyväskylä, P.O. Box. 35, FIN-40351, Jyväskylä, Finland*

[3]*Cyclotron Institute, Texas A&M University, 3366 TAMU, College Station, Texas 77843-3366, USA*

(Received 28 June 2018; published 27 August 2018)

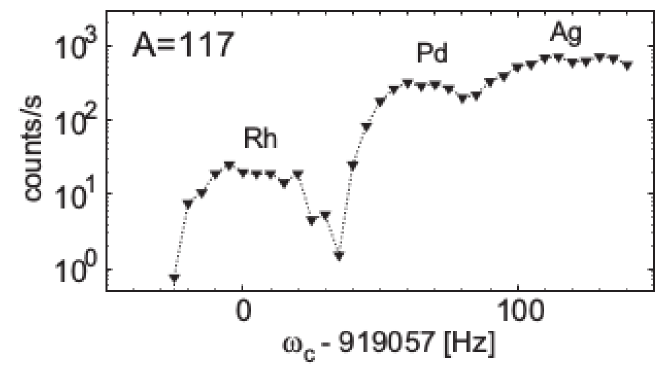

A=117
Rh
Pd
Ag
counts/s
ωc - 919057 [Hz]


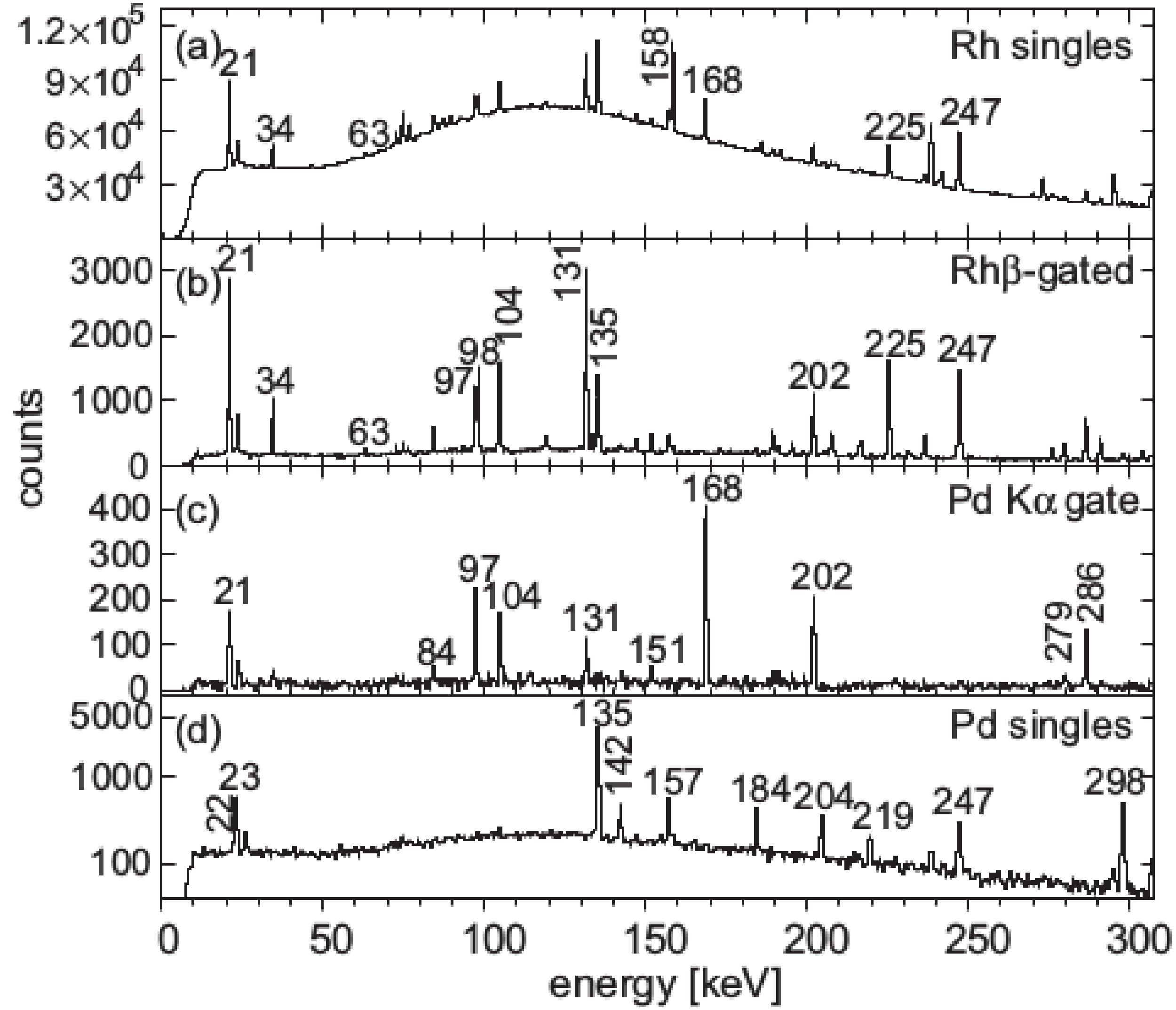

(a)
Rh singles
(b)
Rhβ-gated
(c)
Pd Kα gate
(d)
Pd singles
counts
energy [keV]

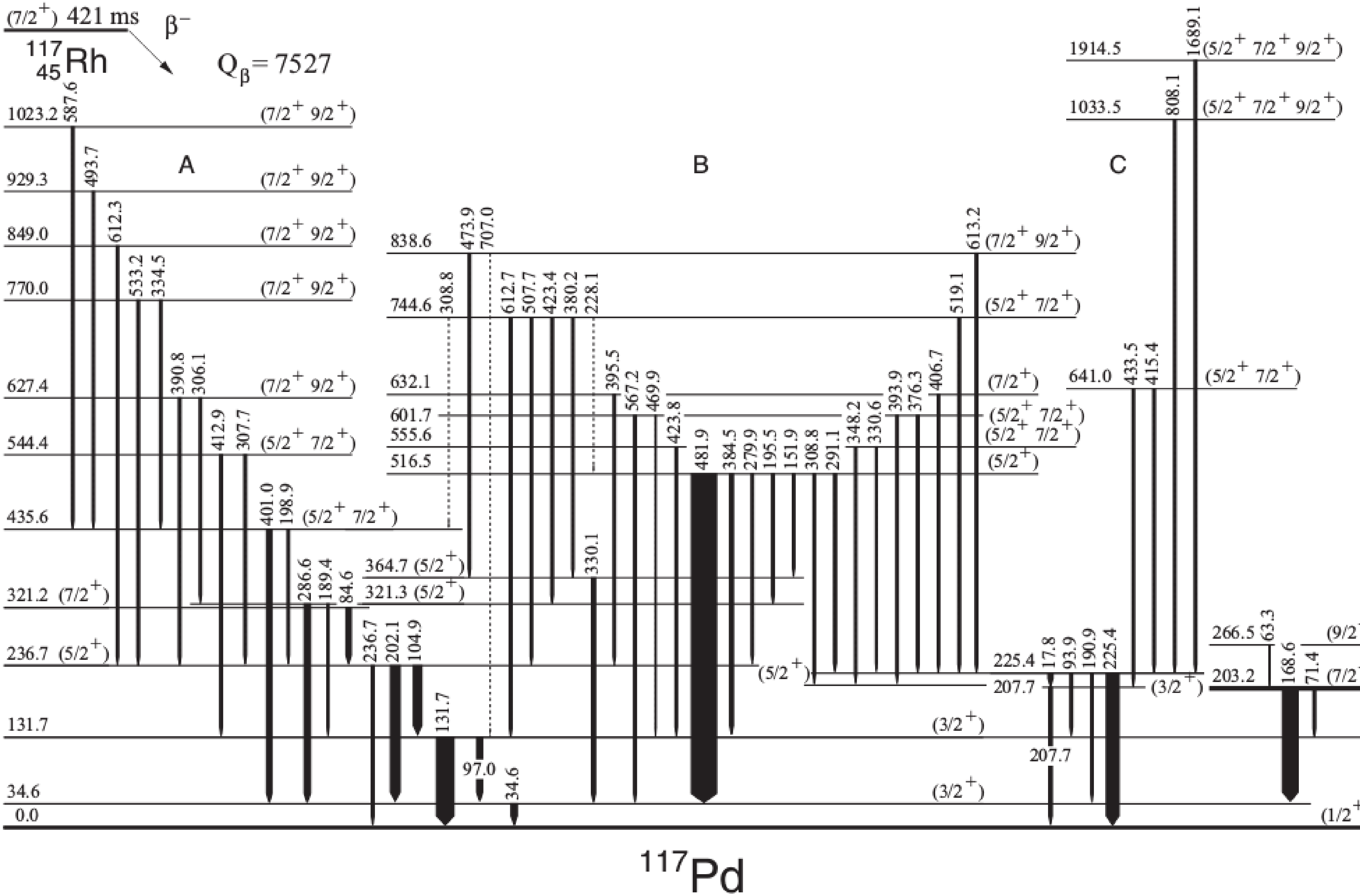

(7/2+) 421 ms
117 45 Rh
β−
Qβ= 7527
A
B
C
1023.2
929.3
849.0
770.0
627.4
544.4
435.6
321.2 (7/2+)
236.7 (5/2+)
131.7
34.6
0.0
(7/2+ 9/2+)
(7/2+ 9/2+)
(7/2+ 9/2+)
(7/2+ 9/2+)
(7/2+ 9/2+)
(5/2+ 7/2+)
(5/2+ 7/2+)
587.6
493.7
612.3
533.2
334.5
390.8
306.1
412.9
307.7
401.0
198.9
286.6
189.4
84.6
236.7
202.1
104.9
131.7
97.0
34.6
838.6
744.6
632.1
601.7
555.6
516.5
364.7 (5/2+)
321.3 (5/2+)
(7/2+ 9/2+)
(5/2+ 7/2+)
(7/2+)
(5/2+ 7/2+)
(5/2+ 7/2+)
(5/2+)
473.9
707.0
308.8
612.7
507.7
423.4
380.2
228.1
330.1
395.5
567.2
469.9
423.8
481.9
384.5
279.9
195.5
151.9
308.8
291.1
348.2
330.6
393.9
376.3
406.7
519.1
613.2
(5/2+)
(3/2+)
(3/2+)
225.4
207.7
17.8
93.9
190.9
225.4
207.7
1914.5
1033.5
641.0
(5/2+ 7/2+ 9/2+)
(5/2+ 7/2+ 9/2+)
(5/2+ 7/2+)
1689.1
808.1
433.5
415.4
(3/2+)
266.5
203.2
63.3
168.6
71.4
(9/2−)
(7/2−)
(1/2+)
117Pd

| $E_{lev}$[keV] | $I_\beta$ | log $ft$ | $E_{lev}$[keV] | $I_\beta$ | log $ft$ |
|---|---|---|---|---|---|
| 0.0 | 0.0 | | 555.6 | 2.9 (0.4) | 6.0 |
| 34.6 | 0.1 (2.1) | 7.8 | 601.7 | 4.3 (0.5) | 5.9 |
| 131.7 | 0 - 4.6 | $\geq$ 6.0 | 627.4 | 1.8 (0.3) | 6.2 |
| 203.2 | $\leq$ 19.2 (1.2) | $\geq$ 5.3 | 632.1 | 2.7 (0.4) | 6.0 |
| 207.7 | 0.0 | | 641.0 | 0.8 (0.2) | 6.6 |
| 225.4 | 3.7 (0.8) | 6.0 | 744.6 | 3.4 (0.4) | 5.9 |
| 236.7 | 7.4 (1.0) | 5.7 | 770.0 | 0.7 (0.1) | 6.6 |
| 266.5 | 1.9 (0.2) | 6.3 | 838.6 | 1.0 (0.3) | 6.4 |
| 321.2 | 5.9 (0.6) | 5.8 | 849.0 | 0.3 (0.1) | 6.9 |
| 321.3 | 2.0 (0.3) | 6.3 | 929.3 | 0.4 (0.1) | 6.8 |
| 364.7 | 1.9 (0.7) | 6.3 | 1023.2 | 0.4 (0.1) | 6.8 |
| 435.6 | 3.2 (0.5) | 6.0 | 1033.5 | 0.4 (0.1) | 6.7 |
| 516.5 | 27.7 (1.7) | 5.1 | 1914.5 | 0.8 (0.1) | 6.2 |
| 544.4 | 2.5 (0.3) | 6.1 | | | |

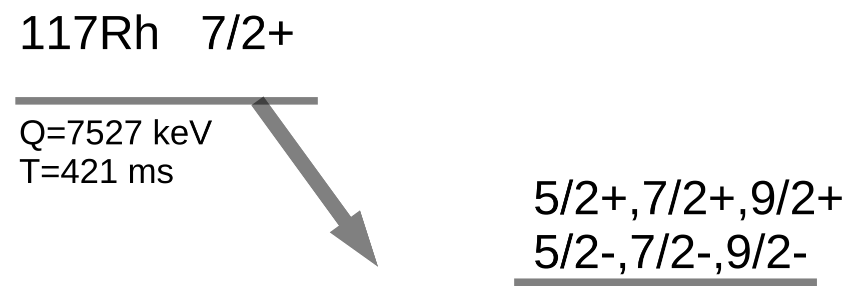


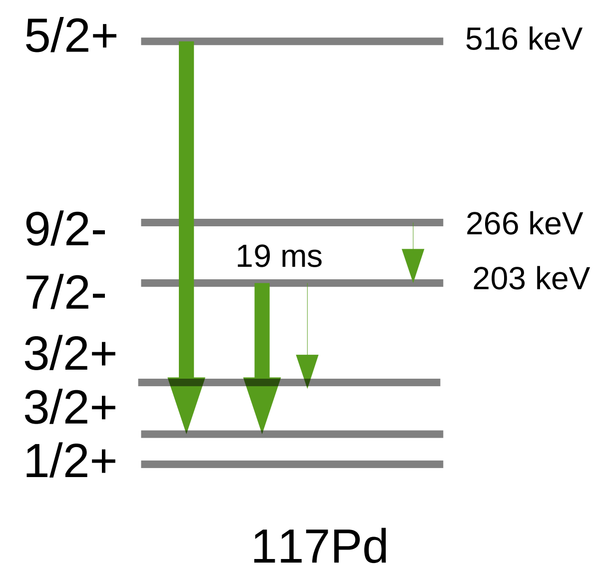


| Izotop | 105Pd | 107Pd | 109Pd | 111Pd | 113Pd | 115Pd | 117Pd |
|---|---|---|---|---|---|---|---|
| Energia poziomu 5/2+ (keV) | 318.9 | 302.7 | 326.9 | 275.4 | 349.1<br>409.2 | 253.8<br>433.4 | 516.5 |
| Log *ft* | 5.1 | 5.0 | 4.9 | 4.8 | 4.9<br>5.3 | 5.0<br>5.3 | 5.1 |

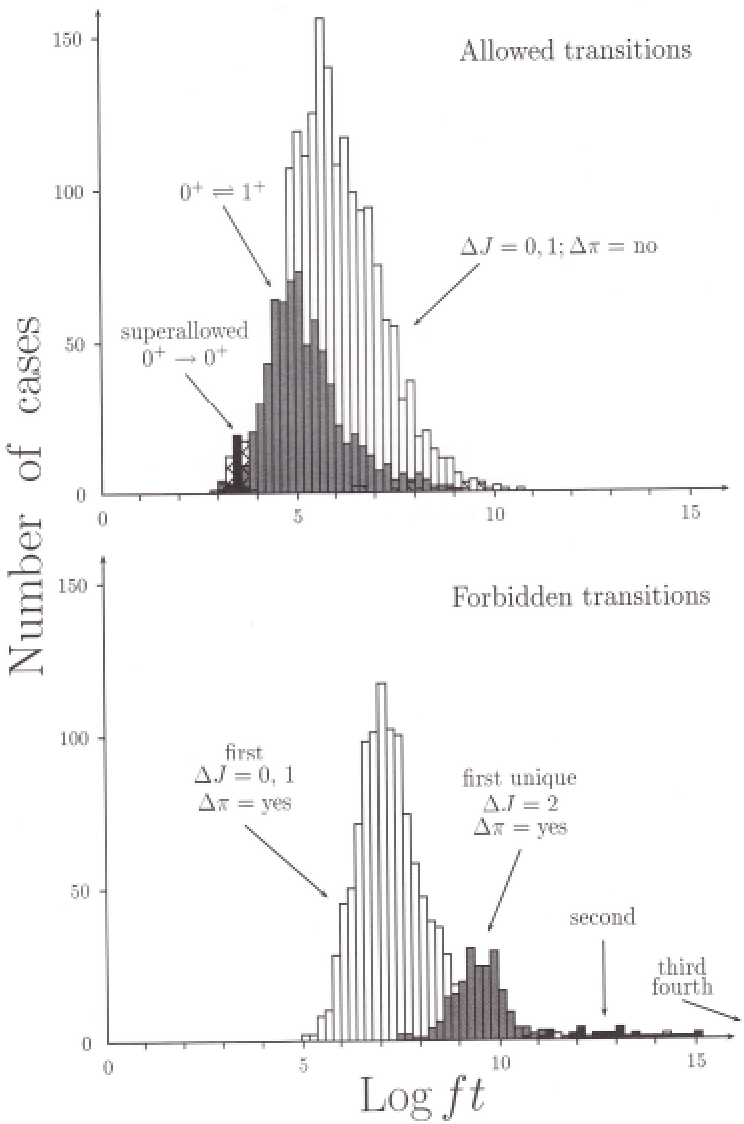


*Nuclear Data Sheets* 84, 487 (1998)
*Article No.* DS980015

# Review Of Log$ft$ Values In β Decay*

**B. SINGH, J. L. RODRIGUEZ**

*Department of Physics and Astronomy*
*McMaster University*
*Hamilton, Ontario L8S 4M1, Canada*

**S. S. M. WONG**

*Department of Physics*
*University of Toronto*
*Toronto, Ontario M5S 1A7, Canada*

**J. K. TULI**

*National Nuclear Data Center*
*Brookhaven National Laboratory*
*Upton, New York 11973, USA*

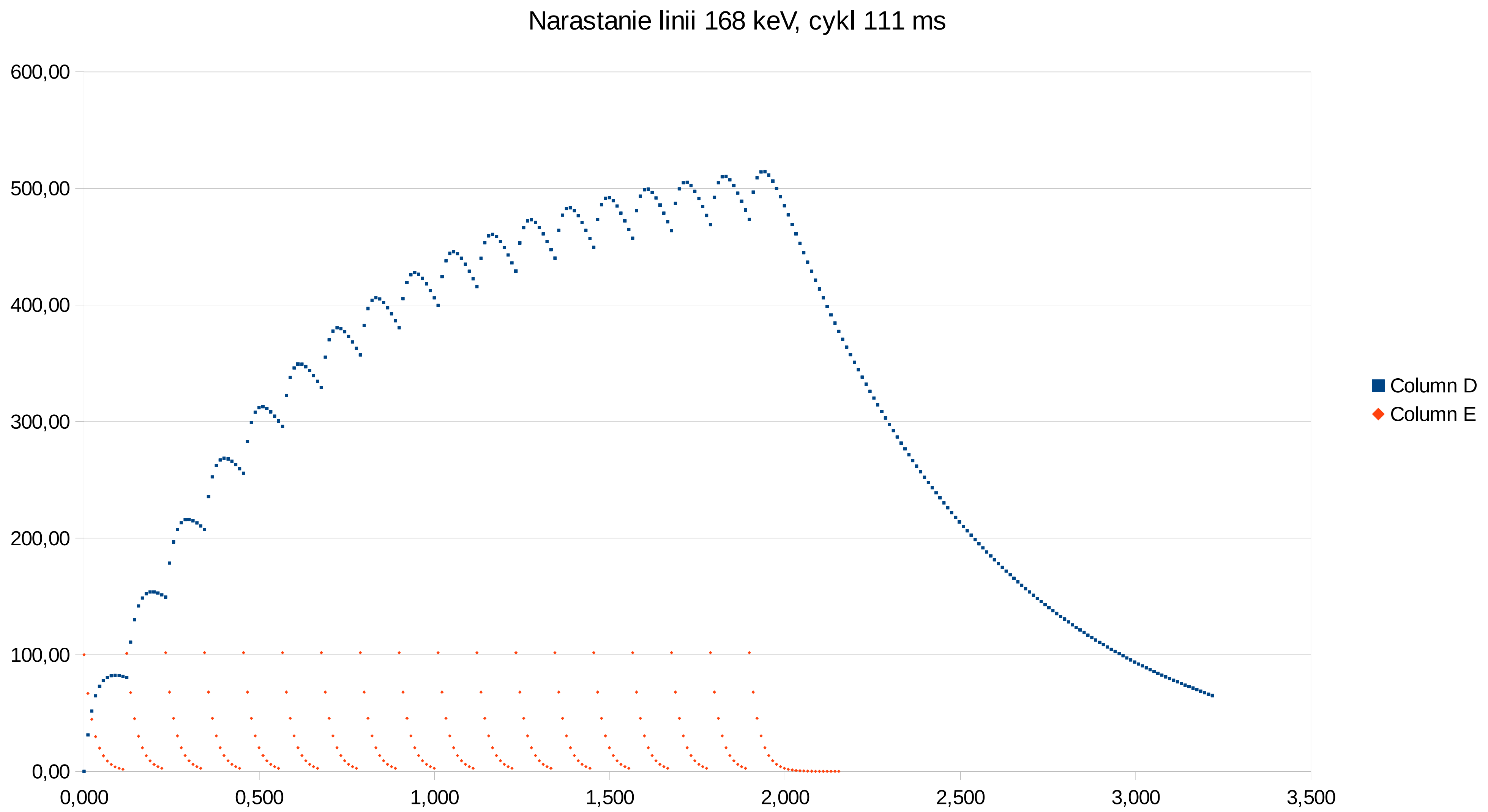
Narastanie linii 168 keV, cykl 111 ms
600,00
500,00
400,00
300,00
200,00
100,00
0,00
0,000
0,500
1,000
1,500
2,000
2,500
3,000
3,500
Column D
Column E

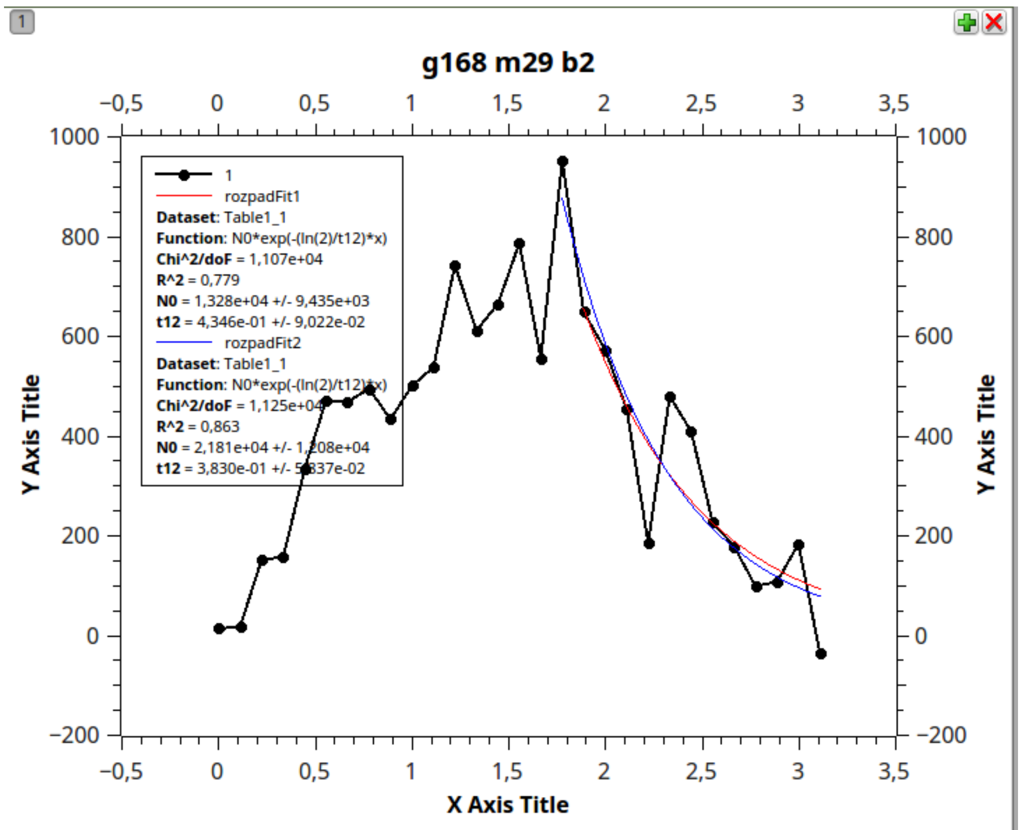
g168 m29 b2
1
rozpadFit1
Dataset: Table1_1
Function: N0*exp(-(ln(2)/t12)*x)
Chi^2/doF = 1,107e+04
R^2 = 0,779
N0 = 1,328e+04 +/- 9,435e+03
t12 = 4,346e-01 +/- 9,022e-02
rozpadFit2
Dataset: Table1_1
Function: N0*exp(-(ln(2)/t12)*x)
Chi^2/doF = 1,125e+04
R^2 = 0,863
N0 = 2,181e+04 +/- 1,208e+04
t12 = 3,830e-01 +/- 5,837e-02
Y Axis Title
X Axis Title

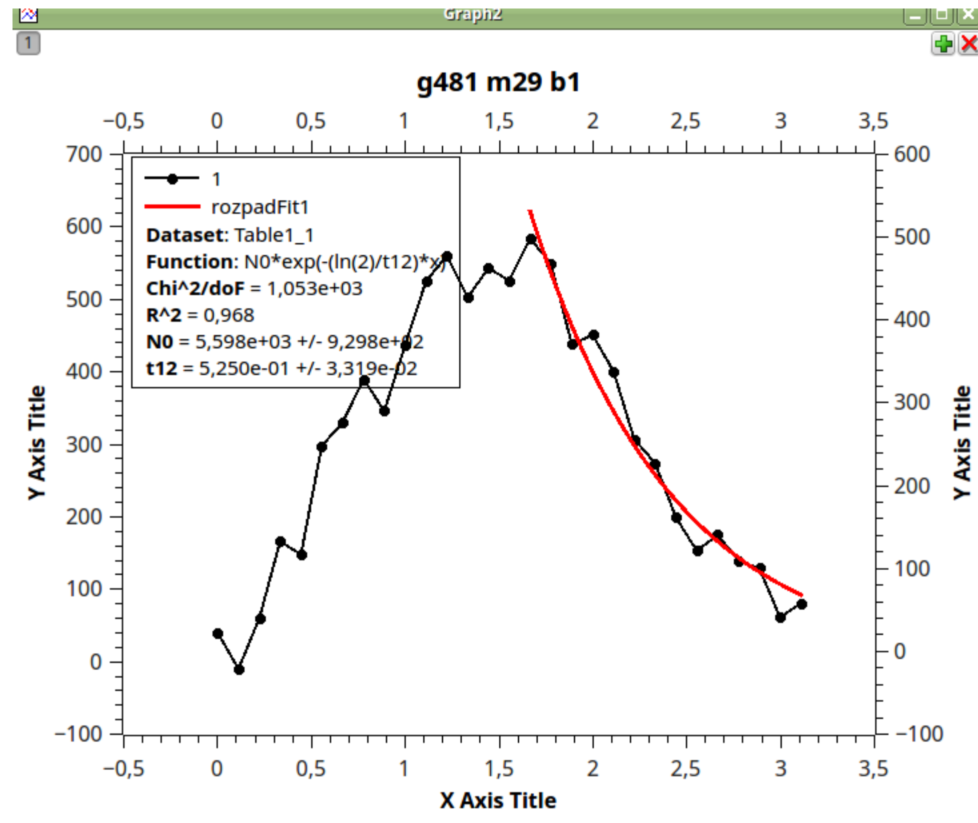
Graph2
g481 m29 b1
1
rozpadFit1
Dataset: Table1_1
Function: N0*exp(-(ln(2)/t12)*x)
Chi^2/doF = 1,053e+03
R^2 = 0,968
N0 = 5,598e+03 +/- 9,298e+02
t12 = 5,250e-01 +/- 3,319e-02
Y Axis Title
X Axis Title

| $E_{lev}$[keV] | $I_\beta$ | log $ft$ | $E_{lev}$[keV] | $I_\beta$ | log $ft$ |
|---|---|---|---|---|---|
| 0.0 | 0.0 | | 555.6 | 2.9 (0.4) | 6.0 |
| 34.6 | 0.1 (2.1) | 7.8 | 601.7 | 4.3 (0.5) | 5.9 |
| 131.7 | 0 - 4.6 | $\geq$ 6.0 | 627.4 | 1.8 (0.3) | 6.2 |
| 203.2 | $\leq$ 19.2 (1.2) | $\geq$ 5.3 | 632.1 | 2.7 (0.4) | 6.0 |
| 207.7 | 0.0 | | 641.0 | 0.8 (0.2) | 6.6 |
| 225.4 | 3.7 (0.8) | 6.0 | 744.6 | 3.4 (0.4) | 5.9 |
| 236.7 | 7.4 (1.0) | 5.7 | 770.0 | 0.7 (0.1) | 6.6 |
| 266.5 | 1.9 (0.2) | 6.3 | 838.6 | 1.0 (0.3) | 6.4 |
| 321.2 | 5.9 (0.6) | 5.8 | 849.0 | 0.3 (0.1) | 6.9 |
| 321.3 | 2.0 (0.3) | 6.3 | 929.3 | 0.4 (0.1) | 6.8 |
| 364.7 | 1.9 (0.7) | 6.3 | 1023.2 | 0.4 (0.1) | 6.8 |
| 435.6 | 3.2 (0.5) | 6.0 | 1033.5 | 0.4 (0.1) | 6.7 |
| 516.5 | 27.7 (1.7) | 5.1 | 1914.5 | 0.8 (0.1) | 6.2 |
| 544.4 | 2.5 (0.3) | 6.1 | | | |

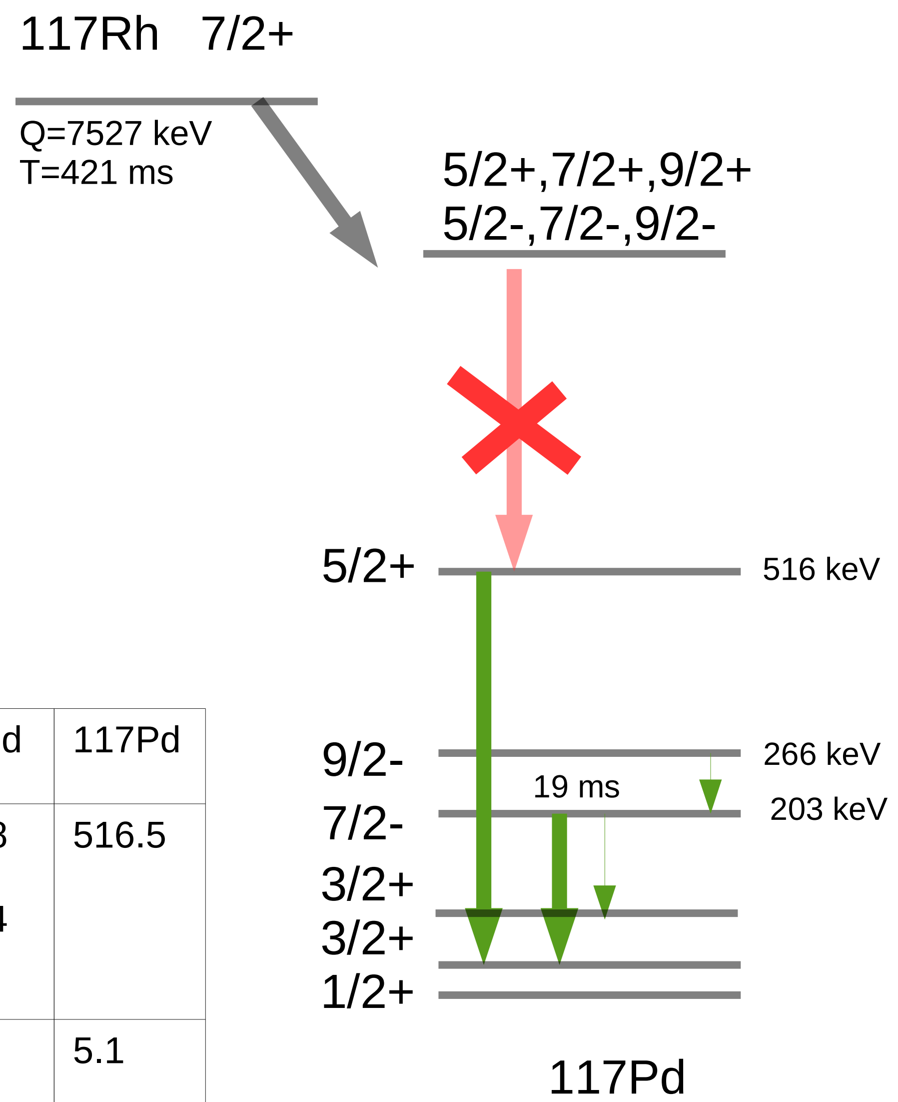


| Izotop | 105Pd | 107Pd | 109Pd | 111Pd | 113Pd | 115Pd | 117Pd |
|---|---|---|---|---|---|---|---|
| Energia poziomu 5/2+ (keV) | 318.9 | 302.7 | 326.9 | 275.4 | 349.1<br>409.2 | 253.8<br>433.4 | 516.5 |
| Log *ft* | 5.1 | 5.0 | 4.9 | 4.8 | 4.9<br>5.3 | 5.0<br>5.3 | 5.1 |

$\Sigma B(GT) = 0.13 – 0.24$

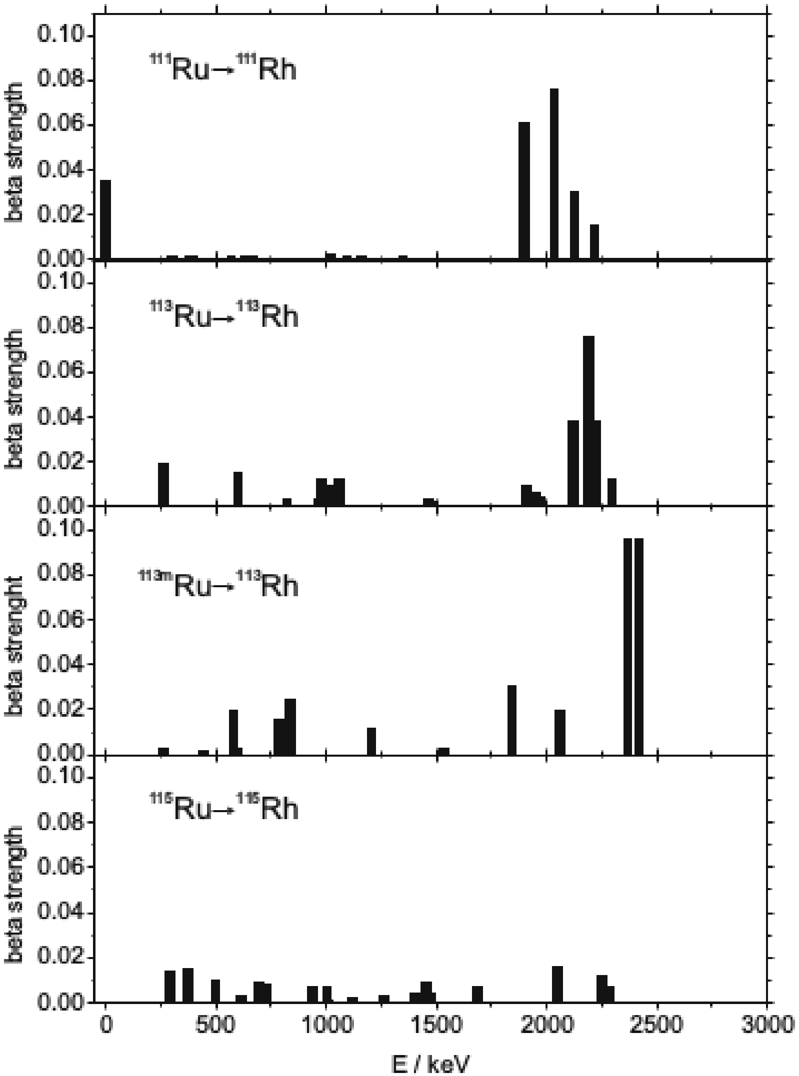


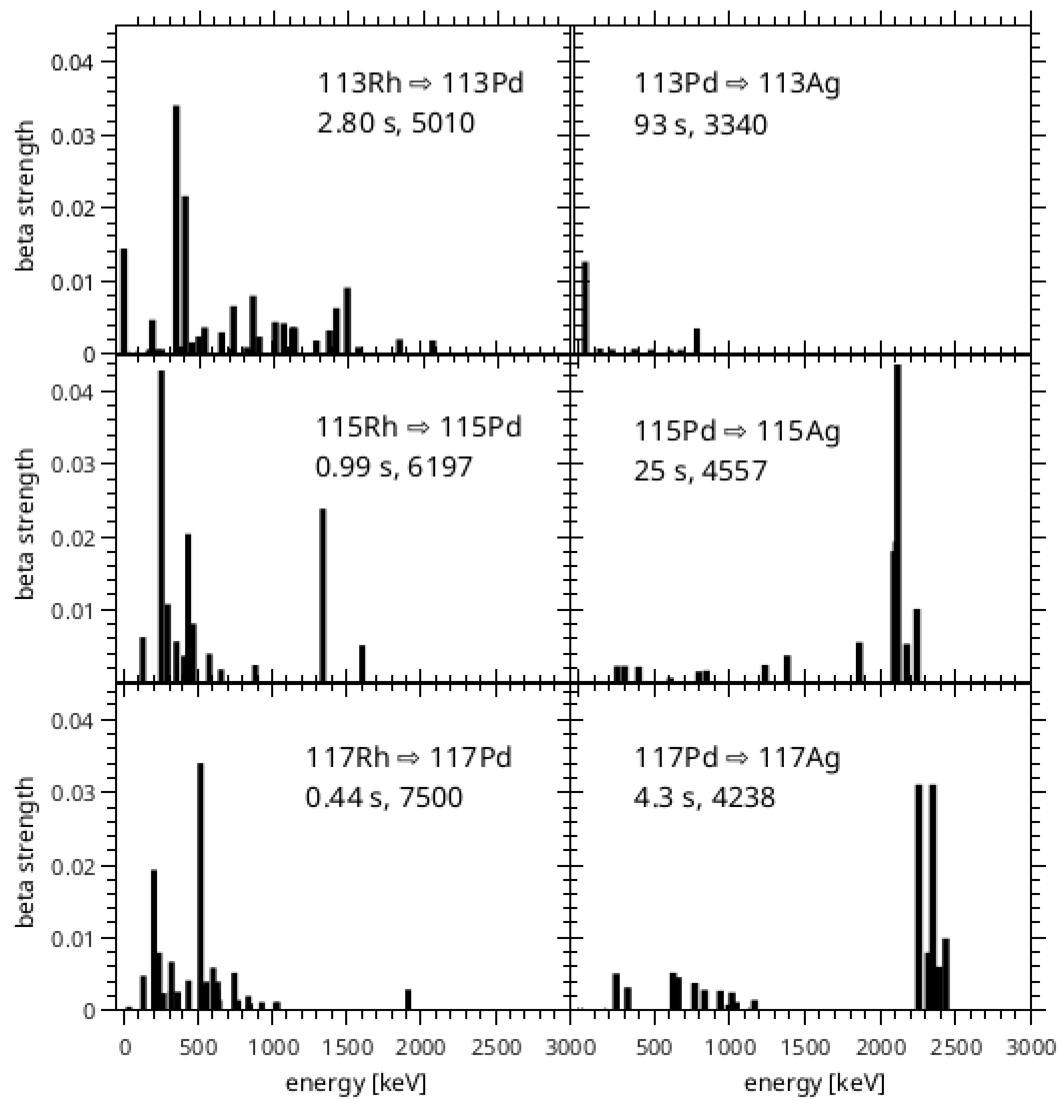


$B_i(GT) = 3860/f_it_i$

BGT

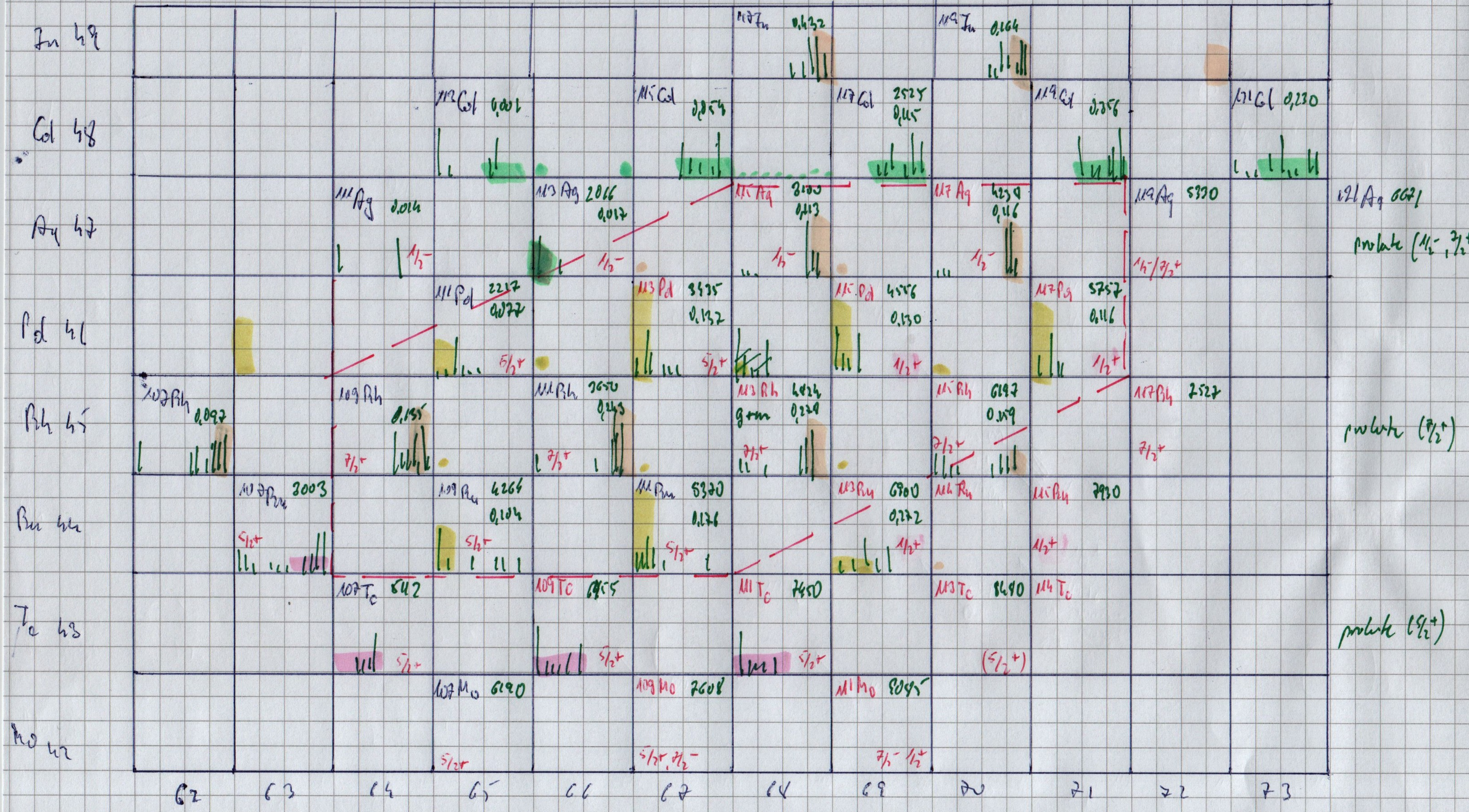

In 49
Cd 48
Ag 47
Pd 46
Rh 45
Ru 44
Tc 43
Mo 42
62
63
64
65
66
67
68
69
70
71
72
73
117In 0,432
119In 0,164
113Cd 0,001
115Cd 0,054
117Cd 2525 0,115
119Cd 0,356
121Cd 0,230
111Ag 0,014
113Ag 2016 0,017
115Ag 3100 0,113
117Ag 4230 0,116
119Ag 5330
121Ag 6671
1/2-
1/2- 7/2+
prolate (1/2-, 7/2+)
111Pd 2217 0,077
113Pd 3435 0,132
115Pd 4556 0,130
117Pd 5757 0,116
5/2+
1/2+
107Rh 0,097
109Rh 0,135
111Rh 3650 0,143
113Rh 4824 0,220
115Rh 6197 0,159
117Rh 7527
7/2+
prolate (7/2+)
107Ru 3003
109Ru 4264 0,104
111Ru 5320 0,176
113Ru 6900 0,272
114Ru
115Ru 7930
5/2+
1/2+
107Tc 5412
109Tc 6455
111Tc 7450
113Tc 8490
114Tc
5/2+
(5/2+)
prolate (5/2+)
107Mo 6190
109Mo 7608
111Mo 8895
5/2+
5/2+, 7/2-
7/2-, 1/2+

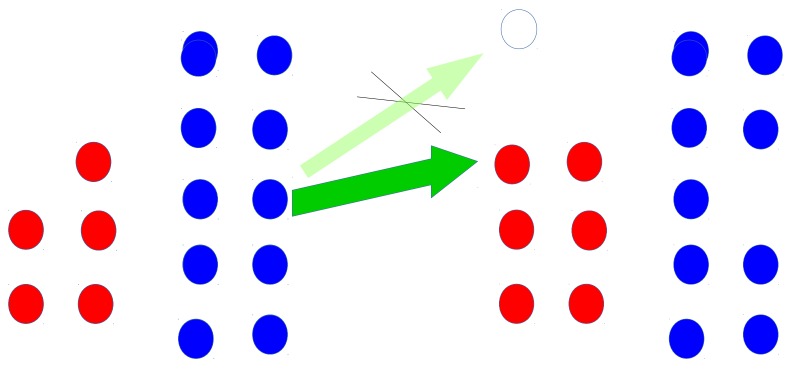

Sparowany neutron zmieniając się w proton zajmuje najniższy stan energetyczny tworząc parę z niesparowanym protonem, stany jądra końcowego są stanami dziur neutronowych. Neutron nie obsadza wyższych stanów protonowych – nie tworzą się stany trój-kwazicząstkowe (2pn). To ma miejsce w rozpadach Rh -> Pd

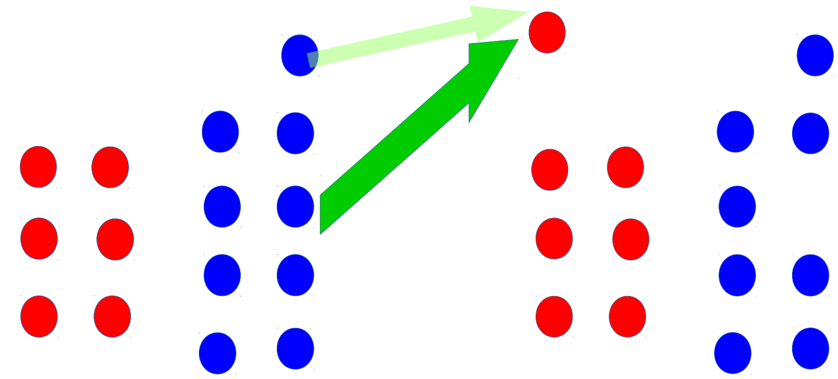

Sparowany neutron zmieniając się w proton zajmuje stan wzbudzony, stany jądra końcowego są stanami trój-kwazicząstkowymi (p2n), ze znacznie mniejszym prawdopodo-bieństwem nieparzysty neutron zamienia się w proton tworząc protonowe stany jednocząstkowe. To zachodzi w rozpadach Ru -> Rh i Pd -> Ag

Co może być przyczyną różnic w obserwowanych rozkładach nasilenia przejść beta?

- brak odpowiednich poziomów – różnice strukturalne
- zbyt wysoka energia poziomów dostępnych do obsadzenia
- duże róznice deformacji

PHYSICAL REVIEW C, VOLUME 65, 021303

Oblate stability of A~110 nuclei near the r-process path

F. R. XU, P. M. WALKER, AND R. WYSS

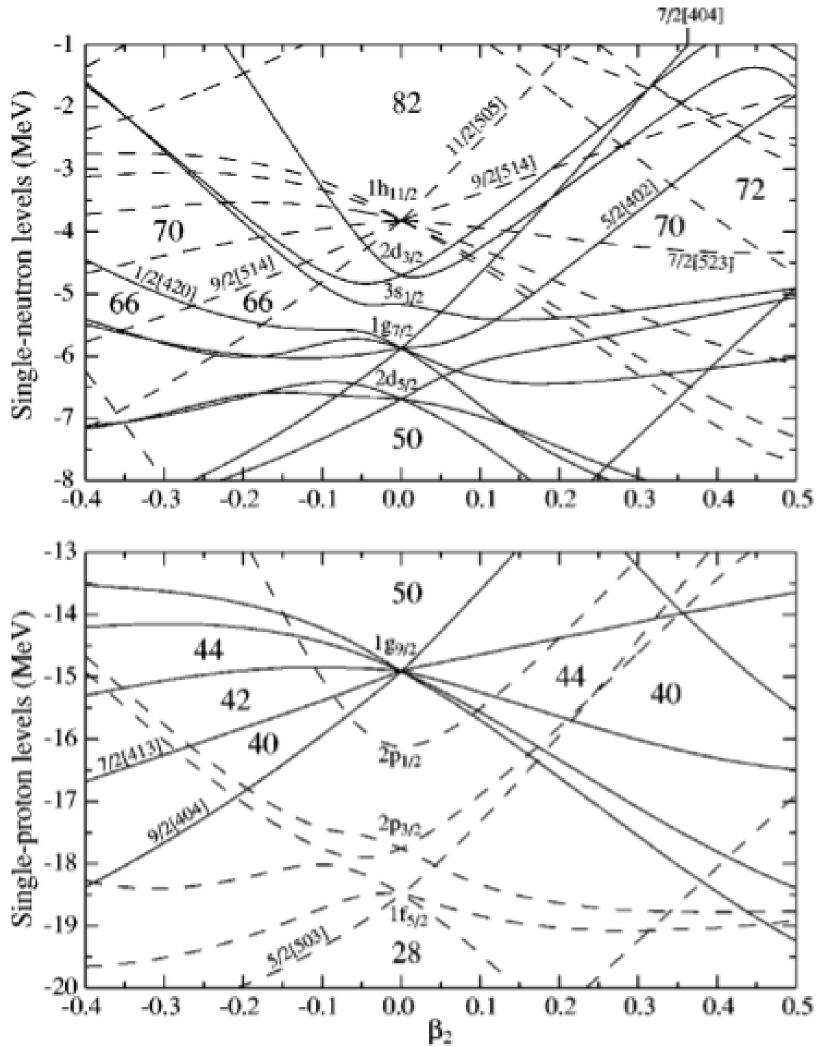


FIG. 1. The calculated single-neutron (top) and single-proton (bottom) levels of the Woods-Saxon potential. Axial symmetry is assumed with $\beta_4 = -|\beta_2|/6$ which gives approximately the hexadecapole value of the ground states obtained from the TRS calculations. Positive (negative) parity is indicated by solid (dashed) lines.

| | 117Rh | 117Pd | 117Ag |
|---|---|---|---|
| $\Delta_n$ | 995 | 1288 | 1087 |
| $\Delta_p$ | 1248 | 951 | 1356 |

| Nuclei | Prolate multi-qp states | | | | | Ground states | | |
|---|---|---|---|---|---|---|---|---|
| | $K^\pi$ | $E_{ex}$ (MeV) | $\beta_2$ | $\beta_4$ | $\lvert\gamma\rvert$ | $\beta_2$ | $\beta_4$ | $\lvert\gamma\rvert$ |
| $^{110}$Zr | $6^-$ | 1.6 | 0.33 | −0.04 | 0° | 0.35 | −0.04 | 0° |
| $^{112}$Zr | $6^-$ | 1.7 | 0.36 | −0.03 | 2° | 0.22 | −0.04 | 60° |
| $^{112}$Zr | $7^-$ | 2.0 | 0.32 | −0.05 | 0° | | | |
| $^{114}$Zr | $7^-$ | 2.7 | 0.36 | −0.04 | 1° | 0.17 | −0.04 | 60° |

| Nuclei | Oblate multi-qp states | | | | Ground states | | |
|---|---|---|---|---|---|---|---|
| | $E_{ex}$ (MeV) | $\beta_2$ | $\beta_4$ | $\lvert\gamma\rvert$ | $\beta_2$ | $\beta_4$ | $\lvert\gamma\rvert$ |
| $^{100}$Se | 1.7 | 0.25 | 0.0 | 59° | 0.29 | −0.03 | 0° |
| $^{102}$Kr | 2.1 | 0.27 | 0.0 | 60° | 0.32 | −0.01 | 0° |
| $^{104}$Sr | 3.0 | 0.25 | −0.01 | 60° | 0.34 | −0.01 | 0° |
| $^{106}$Zr | 2.7 | 0.22 | −0.02 | 63° | 0.34 | −0.02 | 0° |
| $^{108}$Mo | 1.4 | 0.22 | −0.03 | 63° | 0.32 | −0.01 | 18° |
| $^{110}$Ru | 1.4 | 0.23 | −0.03 | 65° | 0.28 | −0.01 | 23° |
| $^{112}$Pd | 1.4 | 0.22 | −0.03 | 65° | 0.25 | −0.02 | 40° |

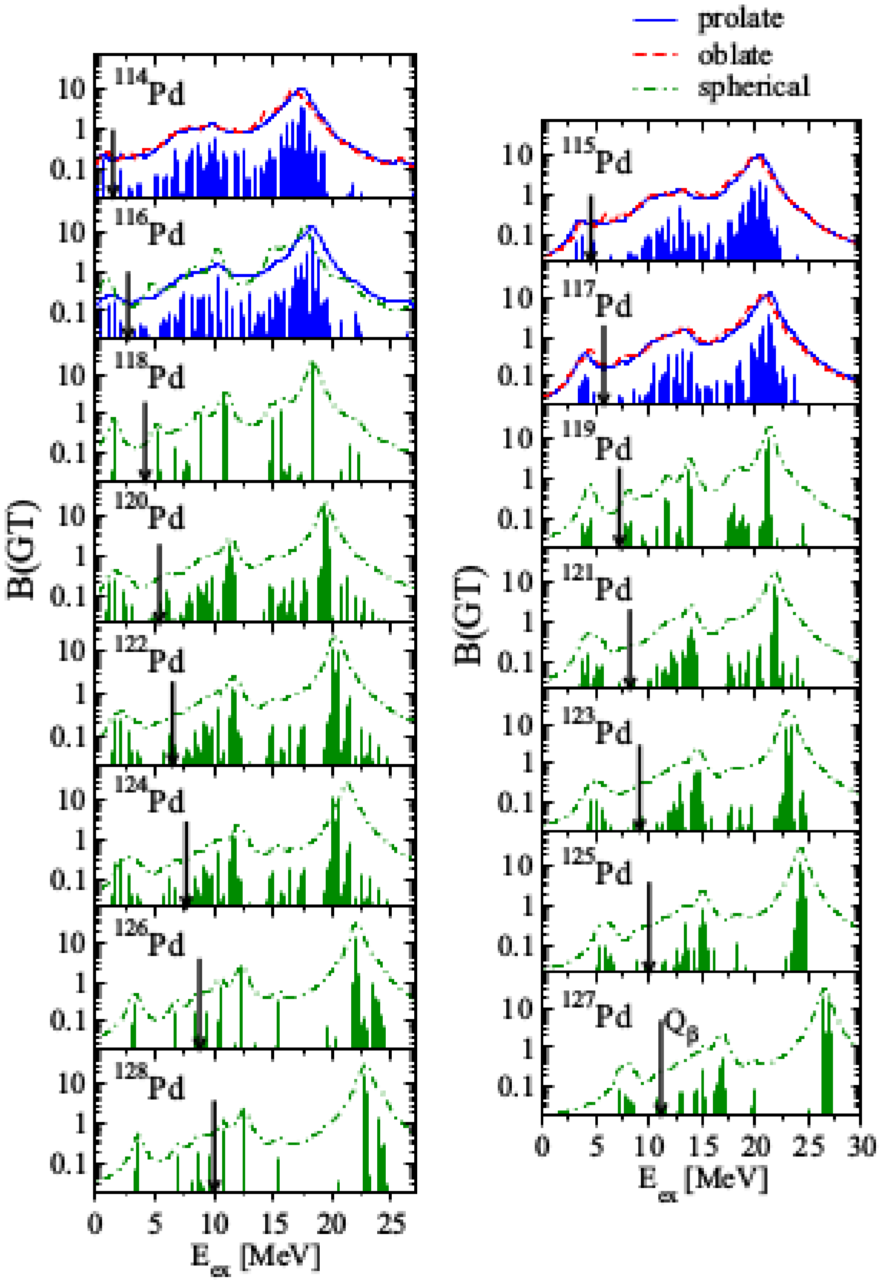
prolate
oblate
spherical
B(GT)
$^{114}$Pd
$^{115}$Pd
$^{116}$Pd
$^{117}$Pd
$^{118}$Pd
$^{119}$Pd
$^{120}$Pd
$^{121}$Pd
$^{122}$Pd
$^{123}$Pd
$^{124}$Pd
$^{125}$Pd
$^{126}$Pd
$^{127}$Pd
$^{128}$Pd
$Q_\beta$
$E_{ex}$ [MeV]

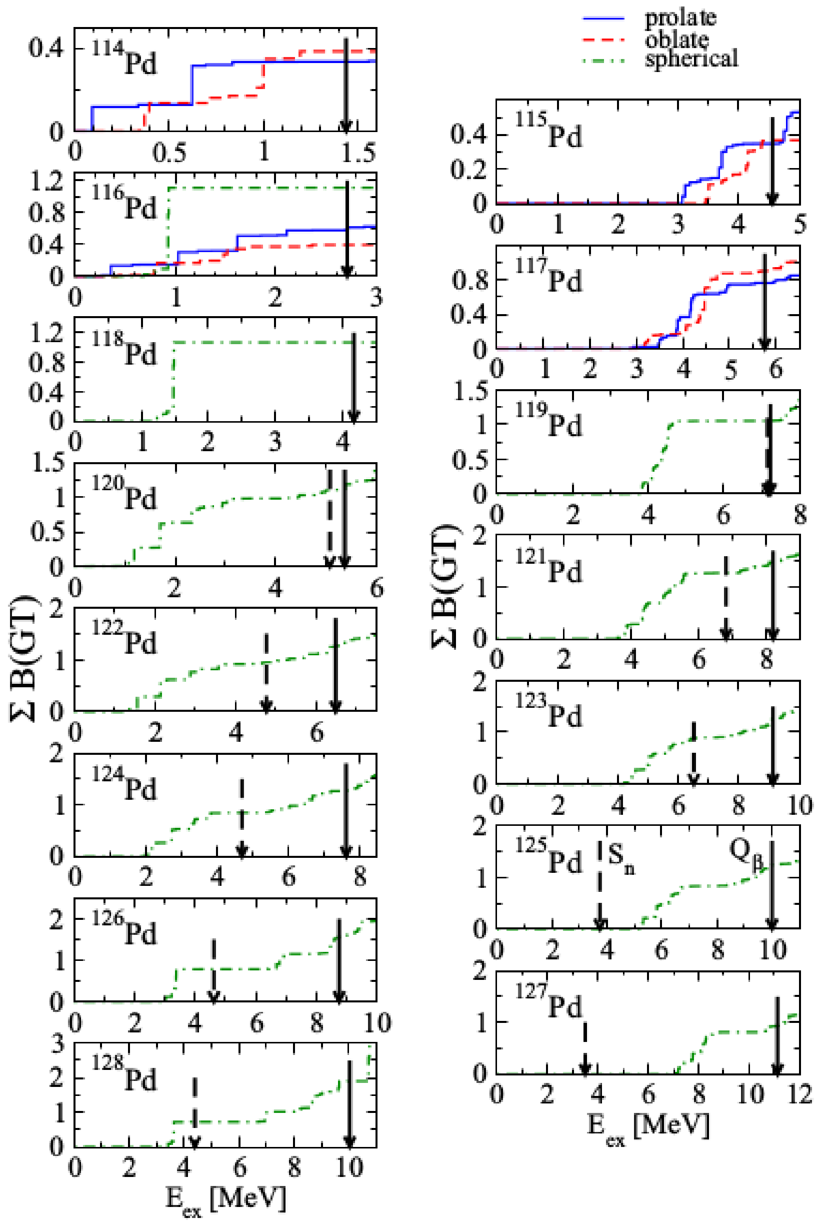
prolate
oblate
spherical
Σ B(GT)
$^{114}$Pd
$^{115}$Pd
$^{116}$Pd
$^{117}$Pd
$^{118}$Pd
$^{119}$Pd
$^{120}$Pd
$^{121}$Pd
$^{122}$Pd
$^{123}$Pd
$^{124}$Pd
$^{125}$Pd
$^{126}$Pd
$^{127}$Pd
$^{128}$Pd
$S_n$
$Q_\beta$
$E_{ex}$ [MeV]

# Stany izomeryczne w nieparzystych izotopach palladu

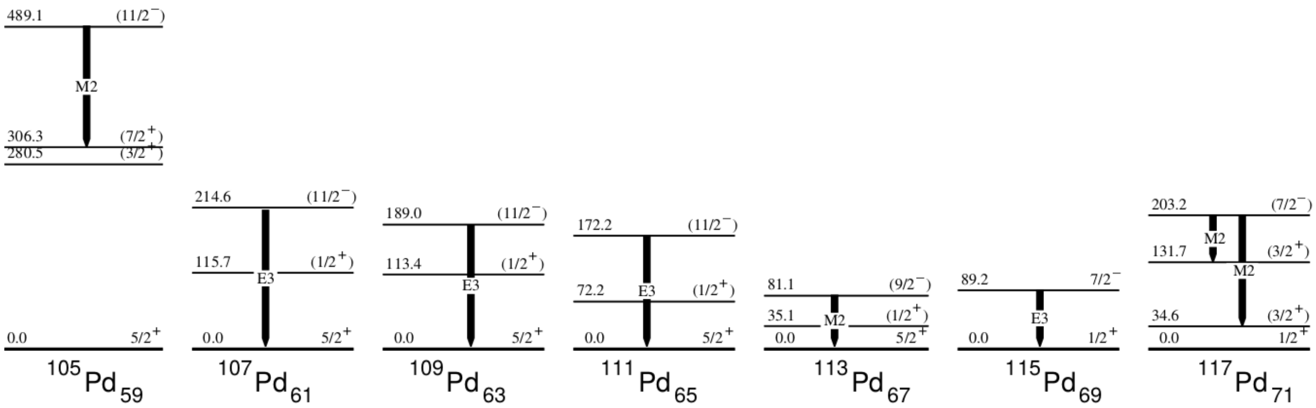


| isotope | $^{105}$Pd | $^{107}$Pd | $^{109}$Pd | $^{111}$Pd | $^{113}$Pd | $^{115}$Pd | $^{117}$Pd |
|---|---|---|---|---|---|---|---|
| mult. | M2 | E3 | E3 | E3 | M2 | E3 | M2<br>M2 |
| hindrance | 7.6 | 379 | 2654 | 165200 | 7590 | 497 | 6780<br>3400 |

$h = \lambda_W / \lambda_{exp}$

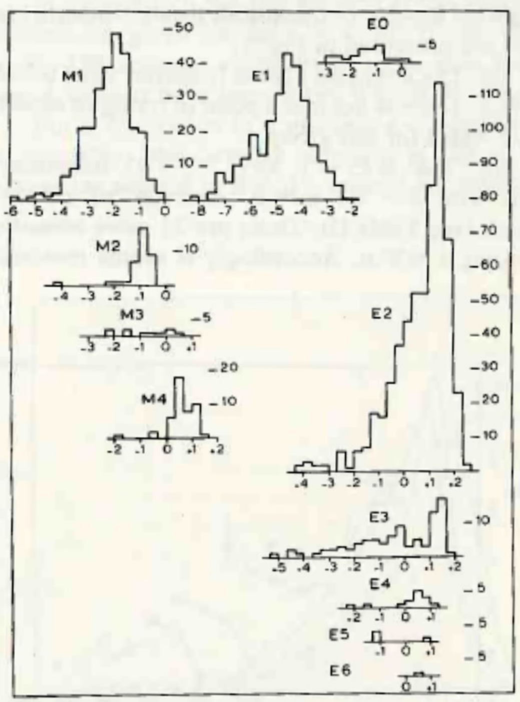


Fig. 1. Gamma-ray strength distributions in the $A = 91$–150 region for transitions of different character ($E0$–$E6$, $M1$–$M4$). The logarithmic abscissa scale indicates the strength in Weisskopf units, except for $E0$ transitions which are in Wilkinson units.

PHYSICAL REVIEW C 91, 044304 (2015)

β-decay properties of neutron-rich Ge, Se, Kr, Sr, Ru, and Pd isotopes from deformed quasiparticle random-phase approximation

P. Sarriguren

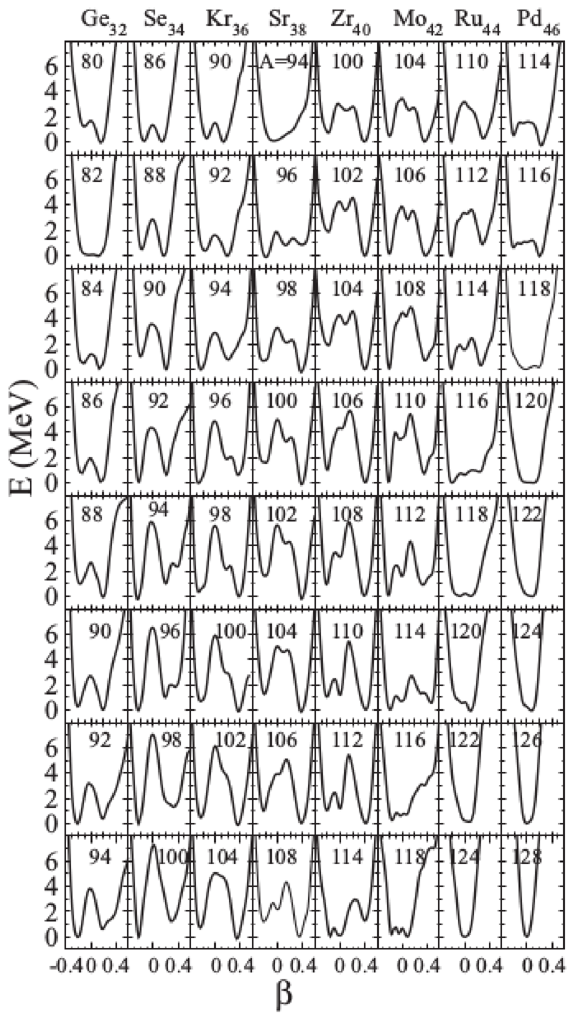


FIG. 1. Potential energy curves for even-even neutron-rich Ge, Se, Kr, Sr, Zr, Mo, Ru, and Pd isotopes obtained from constrained HF + BCS calculations with the Skyrme force SLy4.

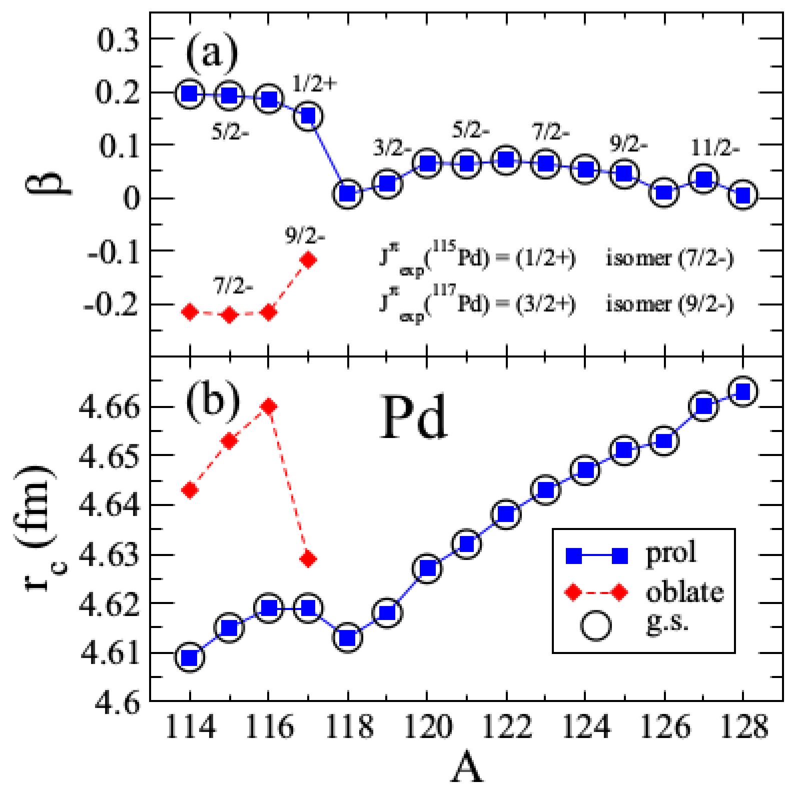

P. Möller, A.J. Sierk, R. Bengtsson, H. Sagawa, T. Ichikawa, Atomic Data and Nuclear Data Tables 98 (2012) 149–300

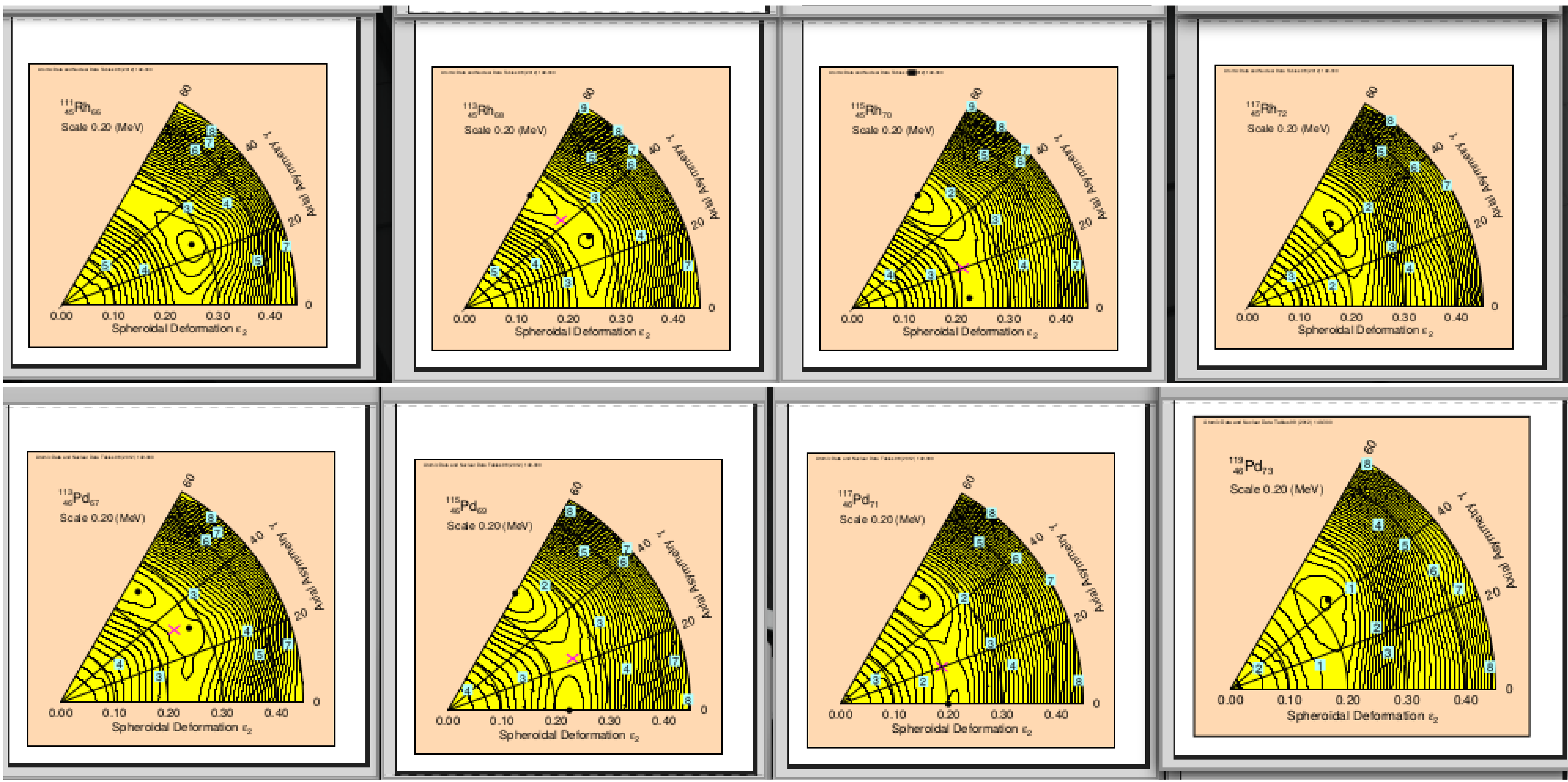

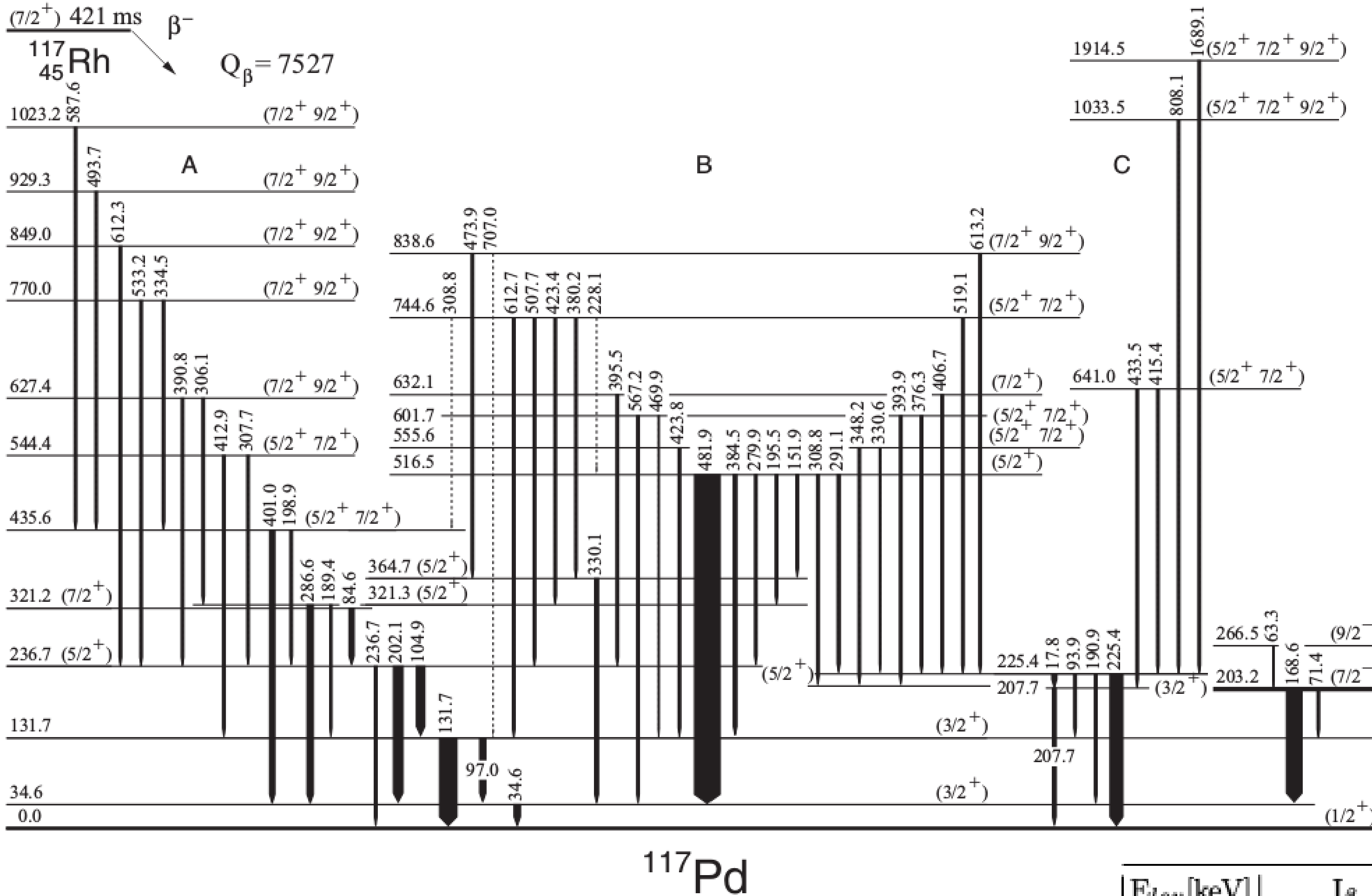


| $E_{lev}$[keV] | $I_\beta$ | log $ft$ | $E_{lev}$[keV] | $I_\beta$ | log $ft$ |
|---|---|---|---|---|---|
| 0.0 | 0.0 | | 555.6 | 2.9 (0.4) | 6.0 |
| 34.6 | 0.1 (2.1) | 7.8 | 601.7 | 4.3 (0.5) | 5.9 |
| 131.7 | 0 - 4.6 | ≥ 6.0 | 627.4 | 1.8 (0.3) | 6.2 |
| 203.2 | ≤ 19.2 (1.2) | ≥ 5.3 | 632.1 | 2.7 (0.4) | 6.0 |
| 207.7 | 0.0 | | 641.0 | 0.8 (0.2) | 6.6 |
| 225.4 | 3.7 (0.8) | 6.0 | 744.6 | 3.4 (0.4) | 5.9 |
| 236.7 | 7.4 (1.0) | 5.7 | 770.0 | 0.7 (0.1) | 6.6 |
| 266.5 | 1.9 (0.2) | 6.3 | 838.6 | 1.0 (0.3) | 6.4 |
| 321.2 | 5.9 (0.6) | 5.8 | 849.0 | 0.3 (0.1) | 6.9 |
| 321.3 | 2.0 (0.3) | 6.3 | 929.3 | 0.4 (0.1) | 6.8 |
| 364.7 | 1.9 (0.7) | 6.3 | 1023.2 | 0.4 (0.1) | 6.8 |
| 435.6 | 3.2 (0.5) | 6.0 | 1033.5 | 0.4 (0.1) | 6.7 |
| 516.5 | 27.7 (1.7) | 5.1 | 1914.5 | 0.8 (0.1) | 6.2 |
| 544.4 | 2.5 (0.3) | 6.1 | | | |

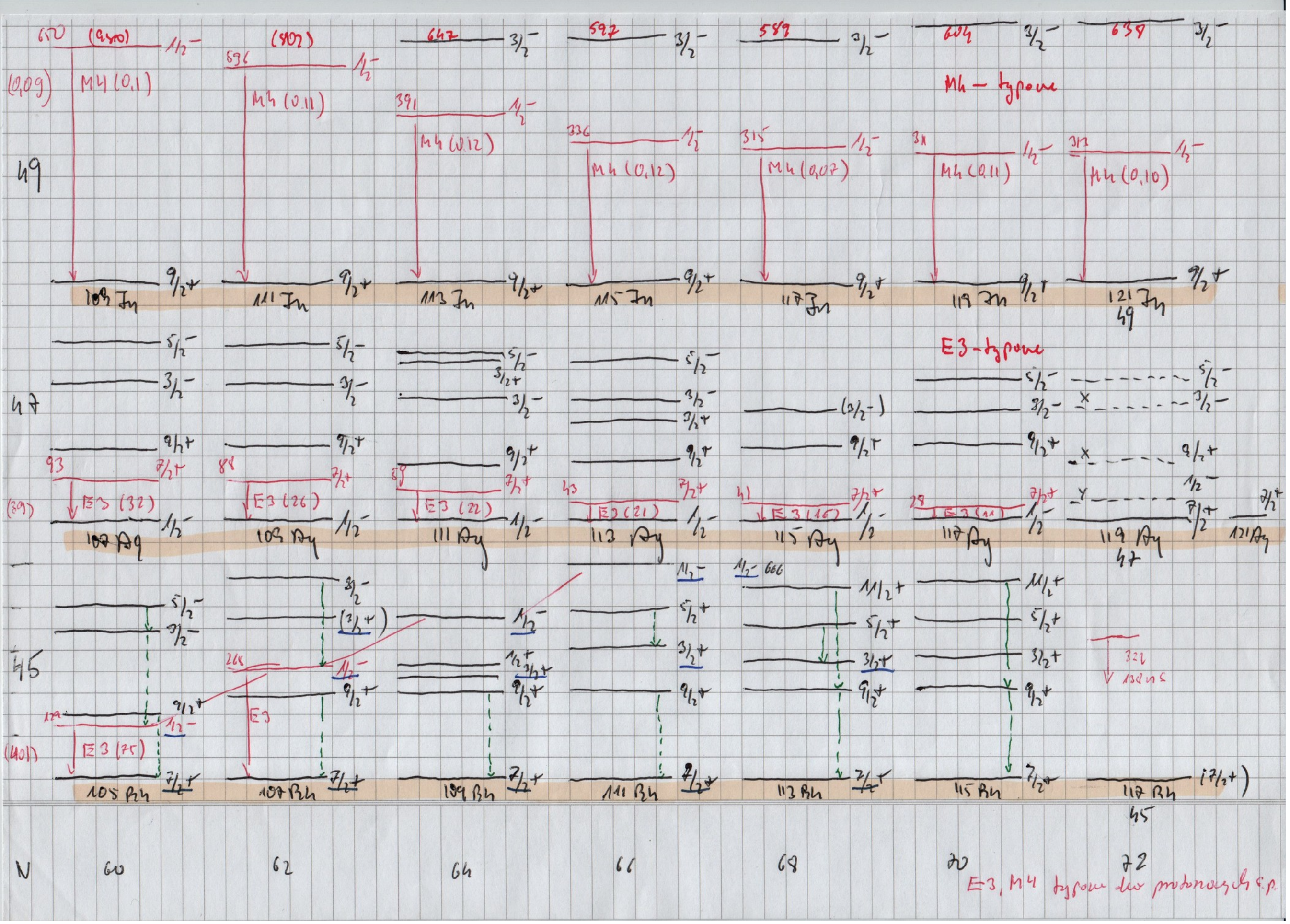




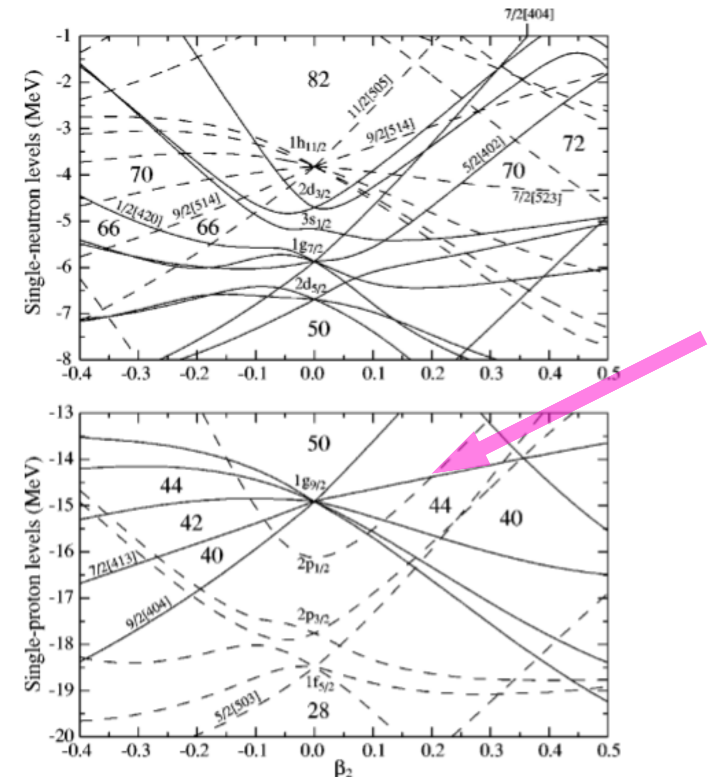


SCIENCE CHINA
Physics, Mechanics & Astronomy
• Article •
September 2016 Vol. 59 No. 9: 692012
doi: 10.1007/s11433-016-0131-7

| Ag Liczba masowa | 107 | 109 | 111 | 113 | 115 | 117 | 119 |
|---|---|---|---|---|---|---|---|
| Energia (keV) 7/2+ -> 1/2- | 93 | 88 | 69 | 43 | 41 | 29 | ? |
| h(E3) | 32 | 26 | 22 | 21 | 16 | 11 | |

**Increased rigidly triaxial deformations in neutron-rich Mo, Ru isotopes**

WuYang Liang[1], ChangFeng Jiao[1], FuRong Xu[1*], and XiMing Fu[2]

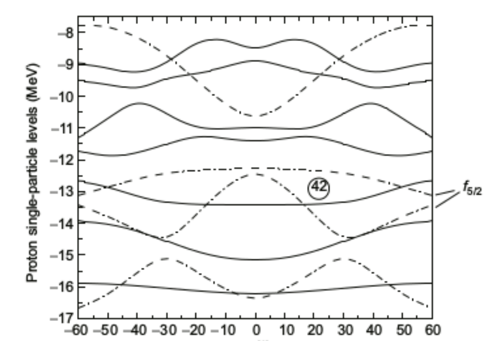


**Figure 5** Calculated WS single-proton levels versus the $\gamma$ deformation. Solid (dot-dashed) curves stand for positive-parity (negative-parity) levels. The calculation is done with fixing $\beta_2$ =0.31 and $\beta_4$ =0.0 (Corresponding to the deformation of the $^{106}$Mo ground state). The proton number of Z=42 is indicated.

PHYSICAL REVIEW C **95**, 064311 (2017)

# Oblate deformation in neutron-rich $^{118,119}$Ag

E. H. Wang,[1] J. H. Hamilton,[1] A. V. Ramayya,[1] Y. X. Liu,[2] H. J. Li,[3] A. C. Dai,[4] W. Y. Liang,[4] F. R. Xu,[4] J. K. Hwang,[1] S. H. Liu,[1] N. T. Brewer,[1,*] Y. X. Luo,[1,5] J. O. Rasmussen,[5] Y. Sun,[6] S. J. Zhu,[3] G. M. Ter-Akopian,[7] and Yu. Ts. Oganessian[7]

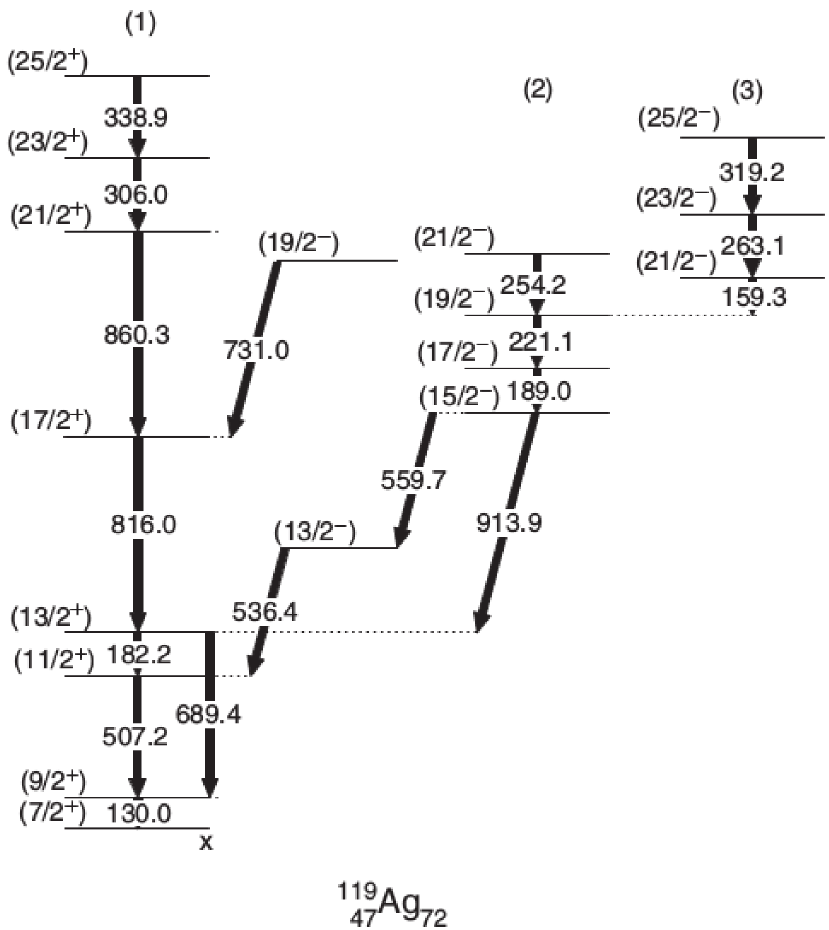


First observation of the beta decay of ll7Pd and the discovery of a new isotope ll9Pd
H. Penttilii , J. Aysto, K. Eskola , Z. Janas , P . P . Jauho , A. Jokinen , M . E . Leino , J. M. Parmonen ,and P. Taskinen
Z. Phys. A - Hadrons and Nuclei 338, 291 (1991)

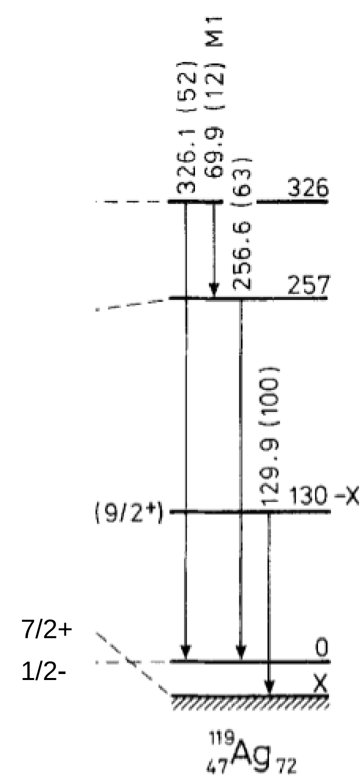

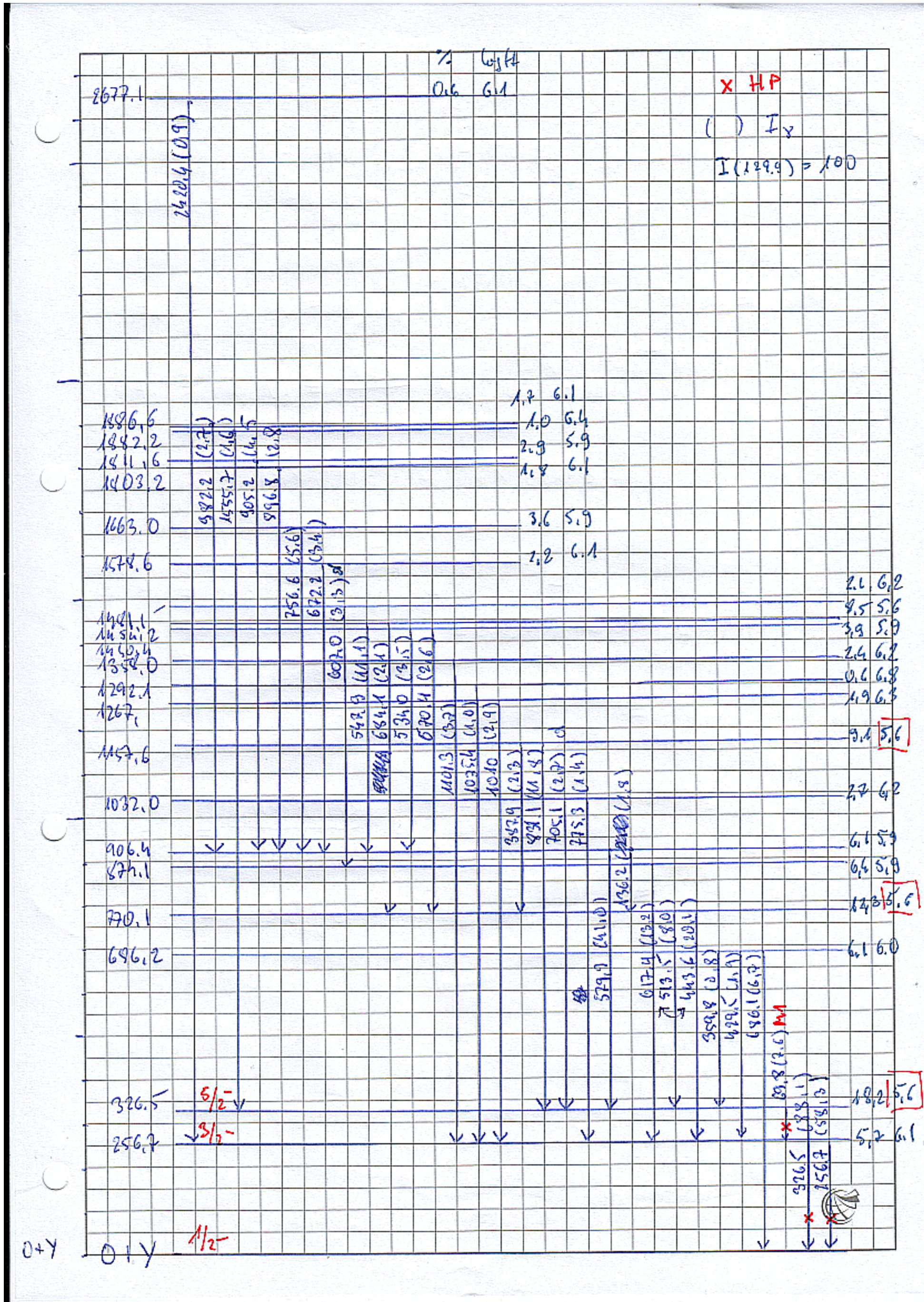
2677.1
% logft
0.6 6.1
× HP
( ) Iγ
I(129.9) = 100
1886.6
1842.2
1811.6
1663.0
1578.6
1032.0
906.4
871.1
770.1
686.2
326.5
256.7
5/2-
3/2-
1/2-
0+Y
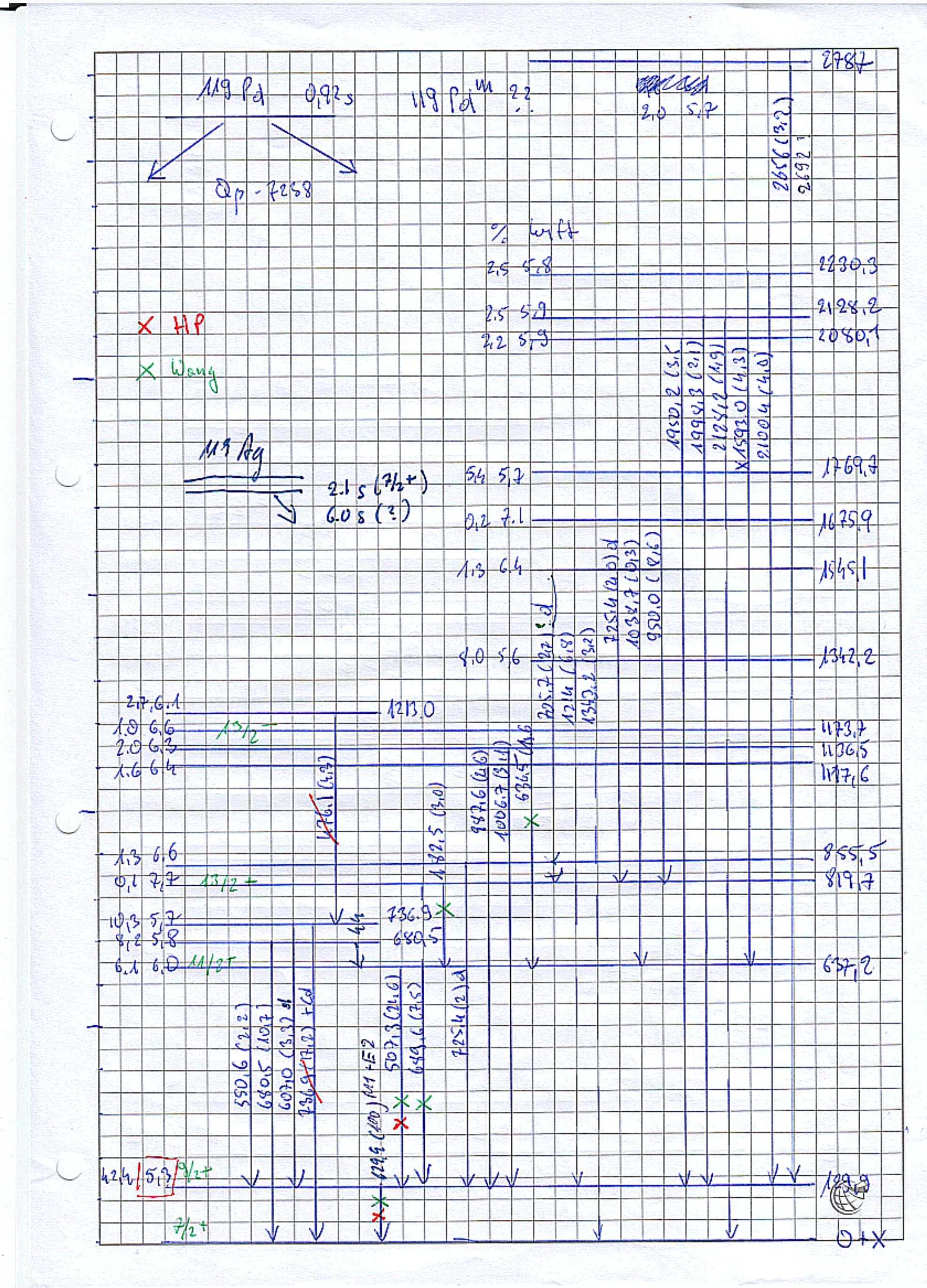
119Pd 0.92 s
Qβ - 7258
% logft
2787
2230.3
2128.2
2080.1
× HP
× Wang
119Ag
2.1 s (7/2+)
6.0 s (?)
1769.7
1675.9
1545.1
1342.2
1213.0
1173.7
1136.5
1117.6
855.5
819.7
13/2+
736.9
680.5
11/2-
637.2
9/2+
129.9
7/2+
0+X

PHYSICAL REVIEW C VOLUME 56, NUMBER 3 SEPTEMBER 1997

# Identification of $^{109}$Mo and possible octupole correlations in $^{107,109}$Mo

J. K. Hwang,[1] A. V. Ramayya,[1] J. H. Hamilton,[1] L. K. Peker,[1] J. Kormicki,[1] B. R. S. Babu,[1] T. N. Ginter,[1] G. M. Ter-Akopian,[1,2,3] Yu. Ts. Oganessian,[2] A. V. Daniel,[1,2,3] W. C. Ma,[4] P. G. Varmette,[4] J. O. Rasmussen,[5] S. J. Asztalos,[5] S. Y. Chu,[5] K. E. Gregorich,[5] A. O. Macchiavelli,[5] R. W. Macleod,[5] J. Gilat,[5,*] J. D. Cole,[6] R. Aryaeinejad,[6] K. Butler-Moore,[6,†] M. W. Drigert,[6] M. A. Stoyer,[7] Y. X. Dardenne,[7] J. A. Becker,[7] L. A. Bernstein,[7] R. W. Lougheed,[7] K. J. Moody,[7] S. G. Prussin,[8] H. C. Griffin,[9] and R. Donangelo[10]

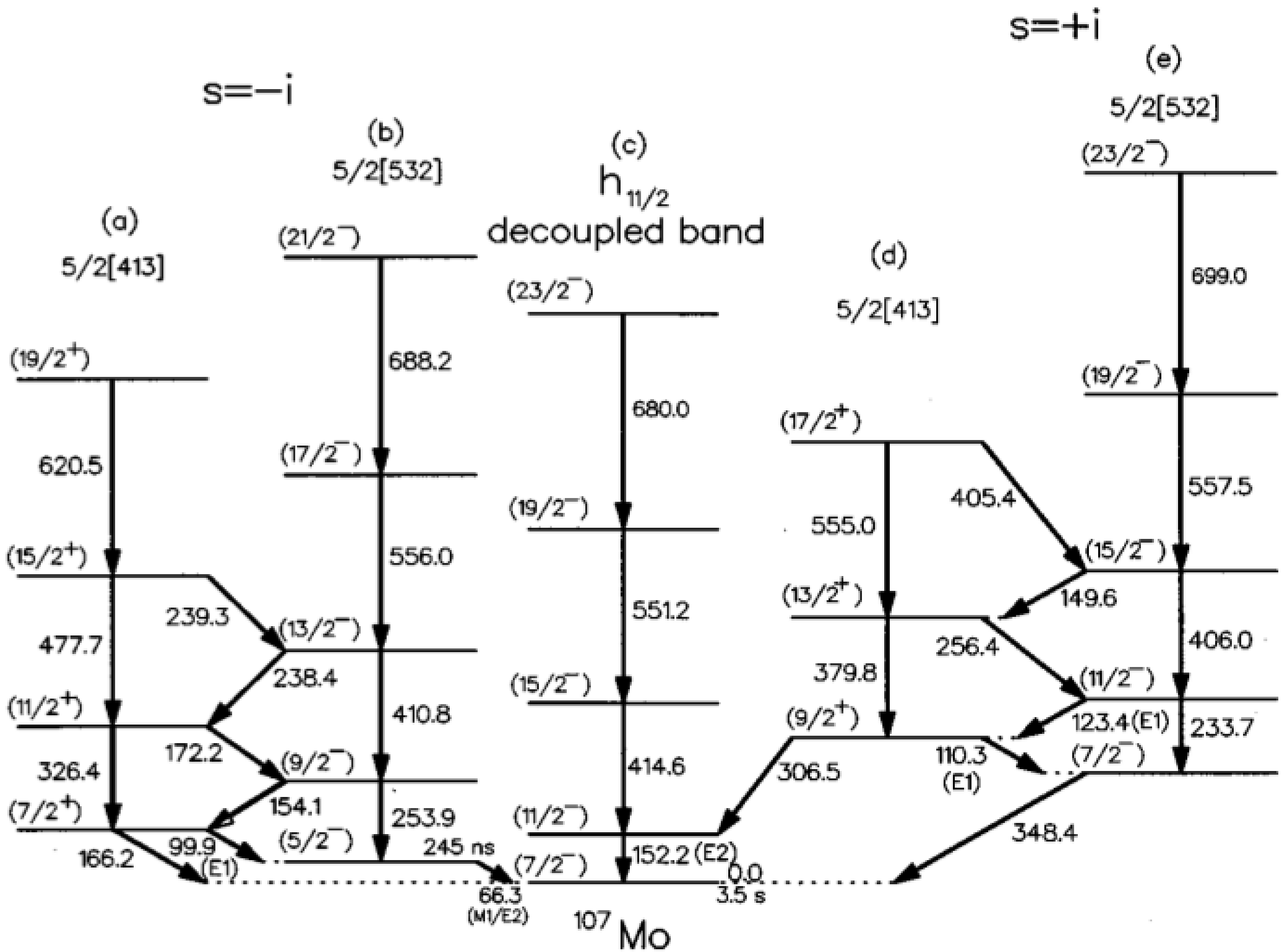

PHYSICAL REVIEW C **69**, 014317 (2004)

# Triaxiality and the aligned $h_{11/2}$ neutron orbitals in neutron-rich Zr and Mo isotopes

H. Hua, C. Y. Wu, D. Cline, A. B. Hayes, and R. Teng
*Nuclear Structure Research Laboratory, Department of Physics, University of Rochester, Rochester, New York 14627, USA*

R. M. Clark, P. Fallon, A. Goergen, A. O. Macchiavelli, and K. Vetter
*Nuclear Science Division, Lawrence Berkeley National Laboratory, Berkeley, California 94720, USA*
(Received 6 October 2003; published 30 January 2004)

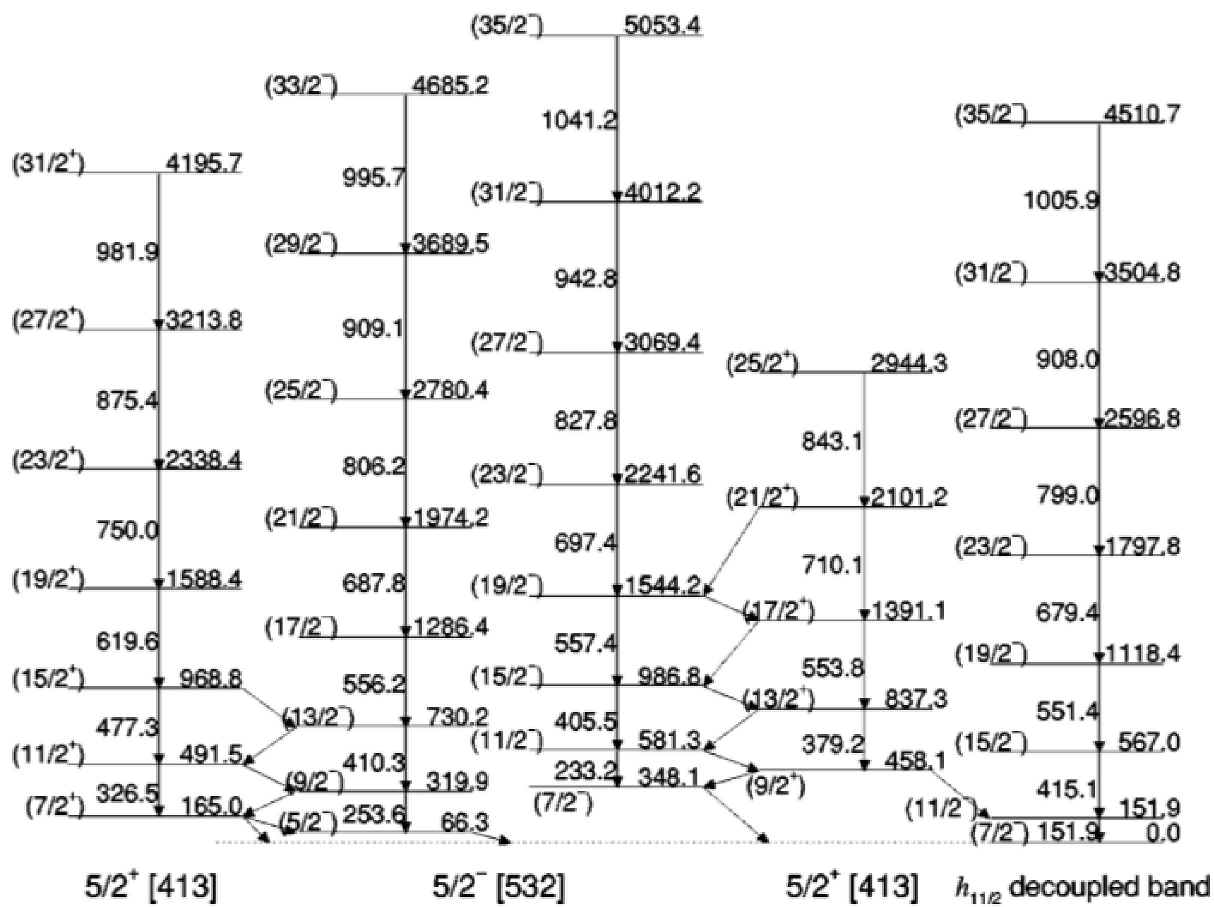

PHYSICAL REVIEW C **72**, 027302 (2005)

## Near-yrast, medium-spin structure of the $^{107}$Mo nucleus

W. Urban,[1] T. Rząca-Urban,[1] J. A. Pinston,[2] J. L. Durell,[3] W. R. Phillips,[3]
A. G. Smith,[3] B. J. Varley,[3] I. Ahmad,[4] and N. Schulz[5]

PHYSICAL REVIEW C **74**, 064304 (2006)

## Triaxiality in $^{105}$Mo and $^{107}$Mo from the low to intermediate spin region

J. A. Pinston,[1] W. Urban,[2] Ch. Droste,[2] T. Rząca-Urban,[2] J. Genevey,[1] G. Simpson,[1] J. L. Durell,[3]
A. G. Smith,[3] B. J. Varley,[3] and I. Ahmad[4]

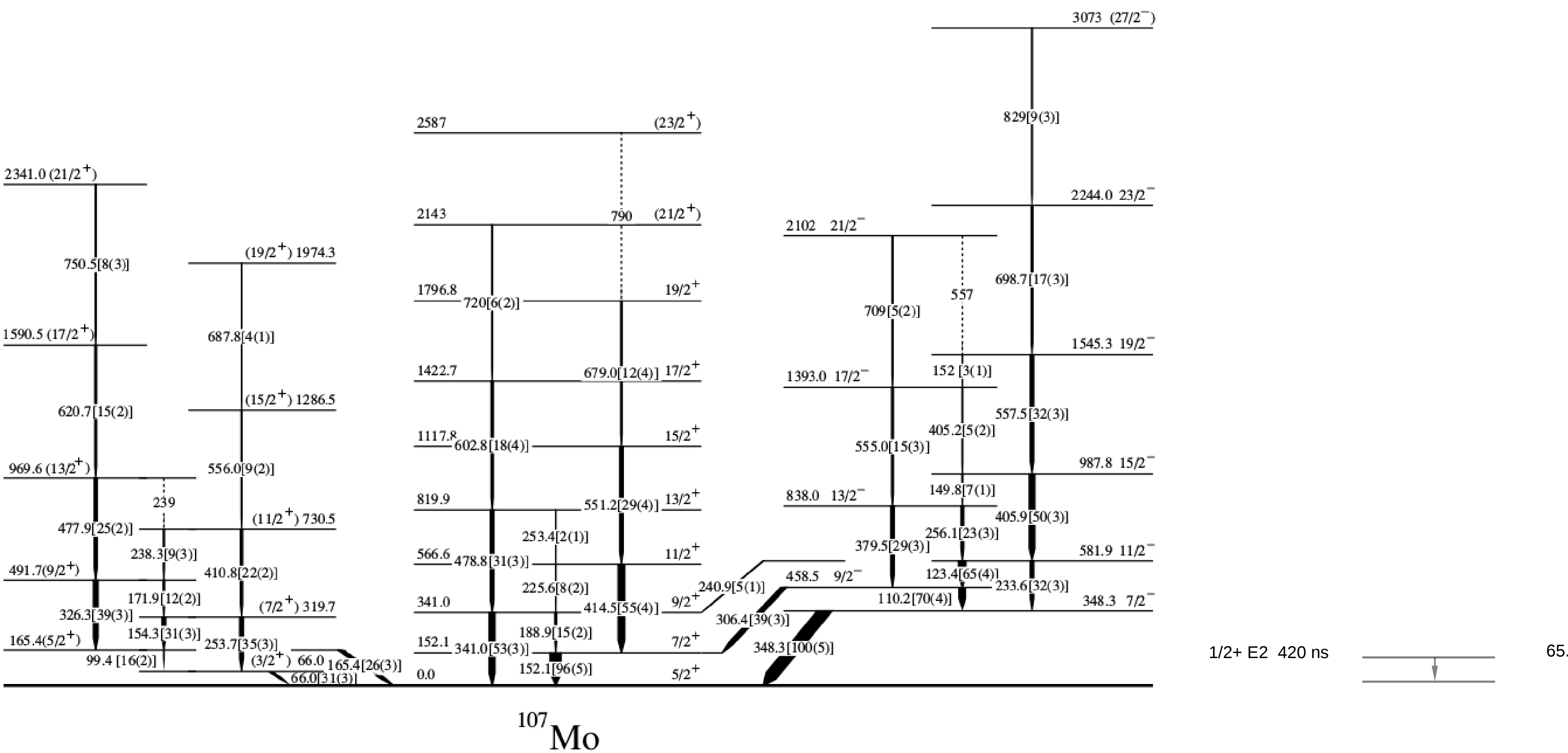

PHYSICAL REVIEW C 96, 034319 (2017)

**One- and two-phonon γ-vibrational bands in neutron-rich $^{107}$Mo**

J. Marcellino,[1,2] E. H. Wang,[1,*] C. J. Zachary,[1] J. H. Hamilton,[1] A. V. Ramayya,[1] G. H. Bhat,[3,4,5] J. A. Sheikh,[4,5] A. C. Dai,[6] W. Y. Liang,[6] F. R. Xu,[6] J. K. Hwang,[1] N. T. Brewer,[1,†] Y. X. Luo,[1,7] J. O. Rasmussen,[7] S. J. Zhu,[8] G. M. Ter-Akopian,[9] and Yu. Ts. Oganessian[9]

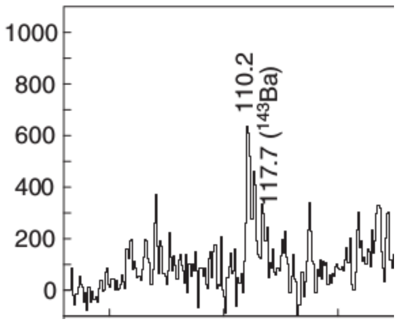


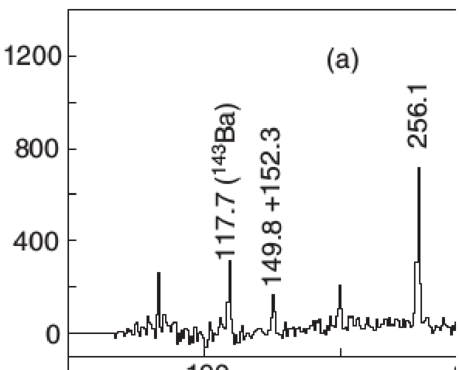


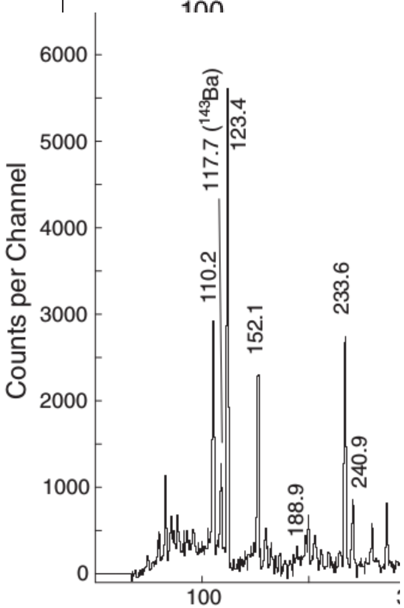


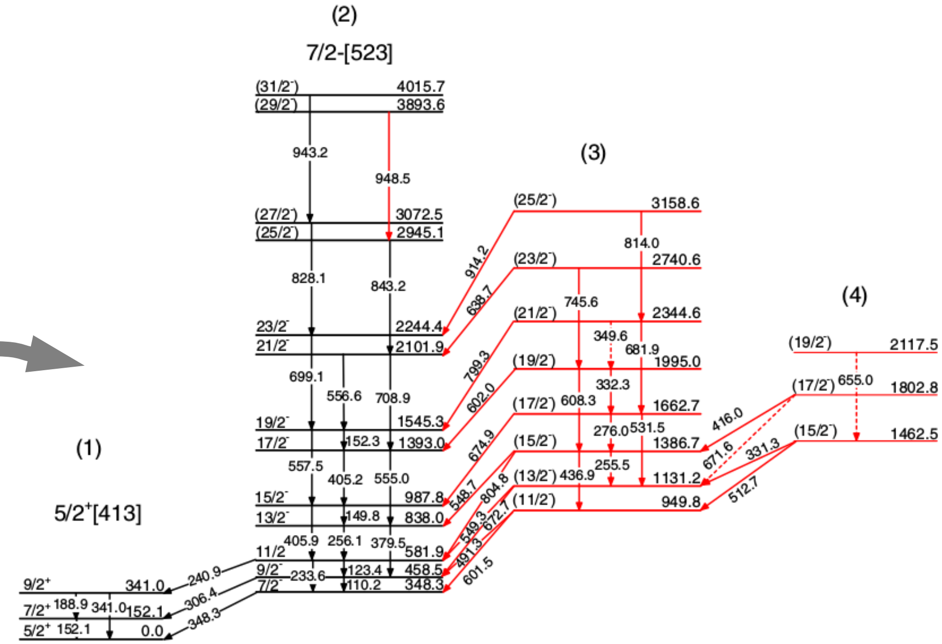


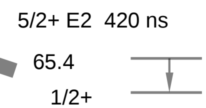


**The first β decay scheme of $^{107}$Nb**

**A new insight into the low-energy levels of $^{107}$Mo**

J. Kurpeta[1], A. Płochocki[1], W. Urban[1], T. Eronen[2], A. Jokinen[2], A. Kankainen[2], I.D. Moore[2], D. Nesterenko[2], H. Penttilä[2], M. Pomorski[1], S. Rinta-Antila[2], and J.A. Niin-Edelen ...

[1] Faculty of Physics, University of Warsaw, ul. Pasteura 5, PL-02-093 Warsaw, Poland
[2] Department of Physics, University of Jyväskylä, P.O.Box. 35, FIN-40351, Jyväskylä, Finland

D. KAMEDA et al.
PHYSICAL REVIEW C 86, 054319 (2012)

| Mo<br>A | 99 | 101 | 103 | 105 | 107 | 109 |
|---|---|---|---|---|---|---|
| g.s.spin | 1/2+ | 1/2+ | (3/2+) | 5/2- | 1/2+ | (1/2+)? |

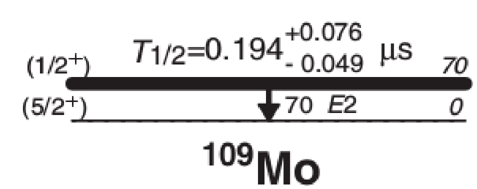

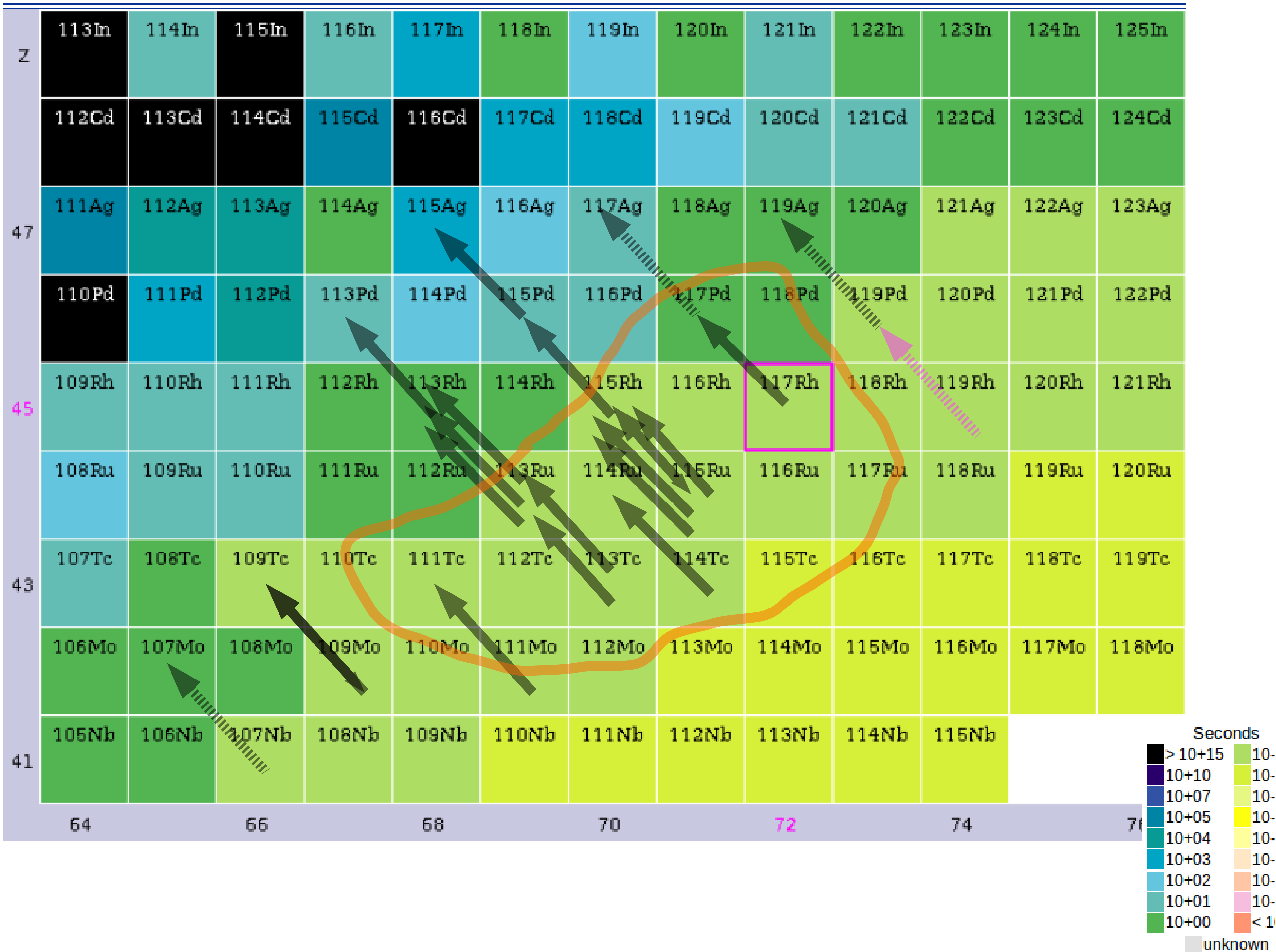

Z
47
45
43
41
113In 114In 115In 116In 117In 118In 119In 120In 121In 122In 123In 124In 125In
112Cd 113Cd 114Cd 115Cd 116Cd 117Cd 118Cd 119Cd 120Cd 121Cd 122Cd 123Cd 124Cd
111Ag 112Ag 113Ag 114Ag 115Ag 116Ag 117Ag 118Ag 119Ag 120Ag 121Ag 122Ag 123Ag
110Pd 111Pd 112Pd 113Pd 114Pd 115Pd 116Pd 117Pd 118Pd 119Pd 120Pd 121Pd 122Pd
109Rh 110Rh 111Rh 112Rh 113Rh 114Rh 115Rh 116Rh 117Rh 118Rh 119Rh 120Rh 121Rh
108Ru 109Ru 110Ru 111Ru 112Ru 113Ru 114Ru 115Ru 116Ru 117Ru 118Ru 119Ru 120Ru
107Tc 108Tc 109Tc 110Tc 111Tc 112Tc 113Tc 114Tc 115Tc 116Tc 117Tc 118Tc 119Tc
106Mo 107Mo 108Mo 109Mo 110Mo 111Mo 112Mo 113Mo 114Mo 115Mo 116Mo 117Mo 118Mo
105Nb 106Nb 107Nb 108Nb 109Nb 110Nb 111Nb 112Nb 113Nb 114Nb 115Nb
64
66
68
70
72
74
Seconds
> 10+15
10+10
10+07
10+05
10+04
10+03
10+02
10+01
10+00
unknown